TOWARDS IMPROVING

BIOFUNCTIONALISATION

BIOFUNCTIONAL LUBRICANT-INFUSED INTERFACES FOR CONTROLLED CELL ADHESION AND PATTERNING

By SARA MOETAKEF IMANI, B.Eng

A Thesis Submitted to the School of Graduate Studies

in Partial Fulfilment of the Requirements for the Degree

Master of Science

McMaster University

McMaster University MASTER OF APPLIED SCIENCE (2017) Hamilton, Ontario (Biomedical Engineering)

TITLE: Biofunctional lubricant-infused interfaces for controlled cell adhesion and patterning

AUTHOR: Sara Moetakef Imani

SUPERVISOR: Dr. Tohid F. Didar

NUMBER OF PAGES: x, 62

Lay Abstract

Biofunctional surfaces, consist of different biomolecules which are immobilized on a desired surface by various means. These surfaces have countless applications in bioengineering, leading to interdisciplinary research, such as lab on chip devices, tissue engineering, diagnostic tools, and medical implants. Therefore, preserving the biofunctionality of the surface as well as preventing non-specific adhesion are required when considering an ideal biofunctional surface. In this work, we designed and developed biofunctional omniphobic lubricant-infused interfaces in order to investigate cell adhesion and non-specific adhesion, simultaneously. This was achieved by producing mixed self-assembled monolayers of organosilanes and also by combining microcontact printing of proteins and self-assembled monolayers of fluorosilanes.

Abstract

Biofunctional surfaces have been under extensive research due to the numerous applications they have in science and technology. In biofunctional surfaces, different biomolecules are immobilized on an interface in order to achieve a stable and selective biorecognition capability. A key characteristic of biofunctional interfaces that is sought after is prevention of non-specific adhesion, which will lead to an improved and selective interaction between the biological elements and the surface as well as reduction of noise in the system.

In this work, we developed biofunctional surfaces which simultaneously have the capability to prevent non-specific binding. For the repellant characteristics, omniphobic liquid-infused coatings were implemented which were developed by producing self-assembled monolayers (SAMs) of fluorosilanes. The biofunctional characteristics were integrated with the interface by two means: (i) producing mixed SAMs of aminosilanes and fluorosilanes to act as a bridge to chemically bind biological recognition elements while simultaneously add omniphobic characteristics, and furthermore, promote controlled biofunctionality (ii) microcontact printing patterns of proteins and further on producing SAMs of fluorosilanes on the surface, therefore resulting in an omniphobic micropatterned biofunctional surface. In order to investigate the biofunctionality, cells specific to the immobilized biomolecules were incubated on the biofunctional lubricant-infused interfaces. Here, we report that by varying the mixed SAMs ratio, we were able to control the degree of cell adherence to the interface. Furthermore, in the case of the micropatterned surfaces, we demonstrated localized cell attachment and enhanced cell specific adhesion.

Acknowledgements

I would like to express my deep gratitude to Dr. Tohid Didar for his guidance and mentorship. Joining Didar Lab and working as a Master's student was truly an honor. Dr. Didar's confidence in my abilities allowed me to become a better and motivated researcher and get closer to my academic goals.

I would like to thank all my friends and colleagues specially, Sara Rahmani, Hanie Yousefi, Sara Jahromi, Azadeh Peivandi, Amid Shakeri, Yasamin Sartipi, Maryam Badv, Mathew Osborne, and Martin Villegas who have always supported me.

Lastly, I would like to express my sincere gratitude and love to my parents, Farzaneh and Behnam. Even though we are apart, their everlasting support and love has given me the power and motivation succeed in life.

Table of Contents

List of figures

Abbreviations

AFM	Atomic Force Microscopy
APTES	3-aminopropyltriethoxy- silane
BSA	Bovine Serum Albumin
BSC	Biosafety Cabinet
CVD	Chemical Vapor Deposition
EDC	N-(3-Dimethylaminopropyl)-N′-ethylcarbodiimide
FITC	Fluorescein Isothiocyanate Isomer I
LOC	Lab on a Chip
LPD	Liquid Phase Deposition
MES	2-(N-Morpholino)ethanesulfonic acid
NHS	N-Hydroxysuccinimide
OEG	Oligo (ethylene glycol)
PBS	Phosphate Buffered Saline
PDMS	Polydimethylsiloxane
PEG	Poly- (ethylene glycol)
PFPP	Perfluoroperhydrophenanthrene
RFP-HUVEC	Red Fluorescent Protein Expressing Human Umbilical Vein Endothelial Cells
SAMs	Self-assembled Monolayers
TPFS	Trichloro (1H,1H,2H,2H-perfluorooctyl) silane
XPS	X-ray Photo Electron Spectroscopy
μCP	Microcontact Printing

Chapter 1 – Introduction

1. Introduction

Surfaces, in general, are critical elements in biomedical and biology related studies. The role of surfaces in biological reactions were initially observed in 19th century and parallel advancements in surface characterization techniques and technology has led to a leap in development of biofunctional surfaces and interdisciplinary research in this field. The properties of the surfaces used in biological interfaces for both *in vitro* and *in vivo* conditions, play a vital role in their biological performance such as protein and cell adhesion and they have been the focus of extensive research for the past few decades. Biofunctional surfaces play a key role in different aspects of science and technology (Castner & Ratner, 2002). Examples of applications for biofunctional surfaces include: medical implants and other blood contacting materials (Petersen et al., 2014; Tan et al., 2013), and biosensors and lab-on-chips (Didar, Foudeh, & Tabrizian, 2012; Liu & Yu, 2016).

In the case of medical implants, research in biofunctional surfaces has led to an enhancement in functions of implants and one of the many examples of implants under research is coronary stents, which are widely used in patients suffering from cardiovascular diseases. Initially, coronary stents where used without any coatings, therefore resulting in complications such as an immunological response of the body, thrombosis, and lack of endothelialisation around the stent. However, engineering stent surfaces have been the focus of research for many years. This has included promoting endothelialisation through coating coronary stents with biomolecules that have affinities against endothelial cells, and/or coatings such as polymers which have the capability to prevent non-specific adhesion (Camci-Unal et al., 2010; Lin et al., 2010; Tan et al., 2013; Yazdani,

Nakano, Otsuka, Kolodgie, & Virmani, 2012). Other examples of medical implants which are widely under research are heart valves, catheters, and vascular grafts (Castner & Ratner, 2002).

Biosensors have also become an immerging field with an exponential trend in the number of publications in the period 1972-2014 (Gonzalez-Rodriguez & Raveendran, 2015). Biosensors can contribute to clinical and diagnostic studies, as well as research and development level in biomedical industries. Biosensors consist of biological recognition elements which are integrated into a transducer. One example of such concept is a biofunctional surface where antigens are immobilized on a surface to detect a corresponding antibody in a sample which further leads to lab-on-a-chip devices (Kasemo, 2002). Other examples of biosensors are devices for blood glucose measurement, infectious disease diagnosis, cancer diagnosis, and single cell cancer detection (Mehrotra, 2016; Turner, 2013). Key elements in biosensing surfaces are selective and stable coupling of biorecognition elements and prevention of non-specific binding, which causes complications in the detection process as well as a reduction in the sensitivity (Gautrot, Huck, Welch, & Ramstedt, 2010; J. Kim, Cho, Seidler, Kurland, & Yadavalli, 2010; Liu & Yu, 2016; Rusmini, Zhong, & Feijen, 2007).

In this work, we set out to develop surfaces which prevent non-specific binding and simultaneously, promote targeted binding by protein immobilization. This technology can further be used as a platform for biosensors or medical implants to overcome the problems mentioned in previous paragraphs. This chapter touches upon current biofunctional surfaces that have implemented non-specific binding approaches and methods of biomolecule immobilization. Following that, methods for covalent and physical immobilization of biomolecules as well as patterning them onto glass surfaces will be discussed. Surface blocking methods and producing self-assembled monolayers (SAMs) of organosilanes will also be discussed.

In the second chapter, a novel approach will be introduced in which mixed SAMs of organosilanes are implemented for both chemical immobilization of proteins and prevention of non-specific binding, as demonstrated by controlled cell adhesion.

The third chapter will detail another novel approach for producing lubricant-infused biofunctional surfaces, using micro-contact printing for patterning proteins and controlling the degree of cell adhesion.

1.1. Biofunctional surfaces

1.1.1. Protein immobilization

Protein immobilization on a solid substrate can be accomplished using several means with regards to the application we are seeking. Traditionally, as shown in many studies, proteins are immobilized through physical adsorption on a desired surface which is a result of hydrophobic and/or electrostatic forces (Rusmini et al., 2007). In this straight-forward approach, proteins are simply incubated on the substrate and the outcome is a surface that has physically-adsorbed proteins immobilized on it. However, this method has some drawbacks such as a high background noise, low sensitivity, less durability, weak attachment, and random orientation.

Chemical adsorption of proteins, which involves covalent binding of proteins on a substrate, is another method for protein immobilization. Generally, the covalent bond is formed between a functional group or coupling agent on the substrate, and the functional groups on the protein. Covalent attachment of protein is durable and furthermore, it can be site-directed which promotes adequate protein activity as it will overcome structural deformation and loss of active functional sites of the protein, thus making it a proper choice for the development of high-performance biosensors (Liu & Yu, 2016; Rusmini et al., 2007).

Depending on the desired application, immobilizing proteins on a surface can be performed with or without a pattern for both chemical and physical immobilization. Patterning proteins provides the advantage of simple detection. For example, in the case of cell capture by proteins, if the capture proteins were immobilized on a surface with a certain pattern, the cells would attach to the surface with the pattern and the assay can be verified by visualizing the pattern. Furthermore, even before cell attachment, the protein immobilization can be verified by different means such as fluorescent microscopy of fluorescently labelled capture proteins or atomic force microscopy (A Bernard, Renault, Michel, Bosshard, & Delamarche, 2000; Zhanga et al., 1999). Surfaces with evenly and homogeneously distributed proteins are also advantageous, for instance, medical implants need to have mostly homogeneous surface characteristics.

Ideally, a potential biofunctional surface with proteins and antibodies should have a proper loading capacity for protein to be immobilized, homogeneous distribution of functional sites, minimum non-specific adhesion, and optimal orientation of the protein for prevention of steric hindrance and exposure of binding sites. An effort for development of a surface with such characteristics will contribute to the fields of biosensors and medical implants. (Liu & Yu, 2016; Trilling, Beekwilder, & Zuilhof, 2013)

1.1.1.1. Chemical immobilization by aminosilanes

In general, organosilanes can act as a bridge between organic and inorganic materials and they are one of the most widely used molecules for this end. Several studies have shown organosilanes as a coupling agent for producing biofunctional surfaces (Lung & Matinlinna, 2012; Zhang et al., 2010). The general configuration for organosilanes is X_3SiRY where X is a group that reacts with the surface (inorganic material) and Y is the organofunctional group (Plueddemann, 1991). Aminosilanes (such as 3-aminopropyltriethoxy-silane (APTES)) are broadly implemented in

biofunctional applications such as controlling cell adhesion and protein adsorption (D. J. Kim, Lee, Park, & Chung, 2011; J. Kim et al., 2010), immunobiosensing surfaces (Awsiuk et al., 2012), as well as producing detection interfaces in lab-on-a-chip (LOC) devices (Didar et al., 2012).

The ethoxy groups in APTES react with a formerly hydroxylated surface, such as glass, and form a siloxane bond (Si-O-Si) where the removal of ethoxy groups produces ethanol. The result of this reaction is a self-assembled monolayer (SAM) of APTES on glass. Liquid phase deposition (LPD) is the most extensively used technique for chemically bonding APTES to a surface (**Figure 1.1**); however, LPD consumes a massive amount of solvent and is reported to produce a less homogeneous and less effective SAM of organosilanes (Badv, Jaffer, Weitz, & Didar, 2017; Zhang et al., 2010). Chemical vapor deposition (CVD) is another method for generating SAMs of APTES which is reported to have greater reproducibility and enhanced homogeneity. Furthermore, the surface is not exposed to impurities that might exist in the liquid phase (Zhang et al., 2010).

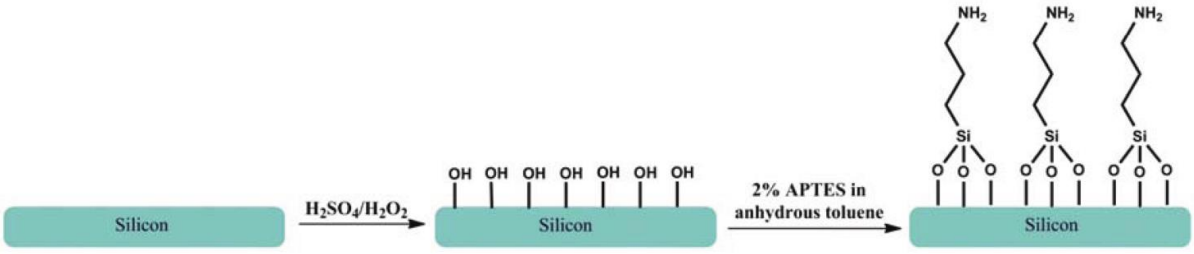

Figure 1.1. Schematic representation of APTES reacting with a hydroxylated surface. Hydroxyl groups are induced on the surface using piranha solution and APTES molecules will chemically bond to the surface in a solution phase reaction. Adapted from (Acres et al., 2012).

The amine terminus of APTES is responsible for the biofunctional characteristics. For instance, through an EDC-NHS chemistry, the amine group of APTES and carboxyl groups of antibodies, go through a chemical reaction which results in a chemically immobilized antibody on the surface (Didar et al., 2012; Petersen et al., 2014).

In this work, we set out to implement APTES as a bridge to chemically bond antibodies to a glass substrate. We modified glass by both CVD and LPD methods, tuned biofunctionality by adjusting the quantity of present APTES in the system, and verified the presence and amount of APTES on the surface using an amine targeting dye, fluorescein isothiocyanate isomer I. Furthermore, after attaching cell specific proteins to the SAM of APTES, cells were cultured on the surfaces to investigate the biofunctionality. The blocking method used for the surfaces is stated in section 1.1.2.3.

1.1.1.2. Physical immobilization by microcontact printing

Microcontact printing was first developed in 1993 in order to create patterns of alkanethiols on gold substrates by stamping an ink of a desired molecule with an elastomer stamp, such as polydimethylsiloxane (PDMS). This opened up a new platform for molecularly and in a micron scale patterning surfaces (Kumar & Whitesides, 1993). The PDMS stamps are fabricated by soft lithography, in such a way that a master mold is created on a silicon wafer using a photoresist and a patterned mask, allowing to have desired patterns on the wafer after being exposed to ultraviolet light. Subsequently, PDMS is dispensed on the mold and cured to generate the stamps.

Patterning proteins on a solid substrate was introduced in 1997 and it has led to numerous research in biosensors and biological applications. A key benefit that microcontact printing of proteins has over other conventional methods, such as photolithography, is that it is relatively easy, has a lower cost, and does not use harsh solvents, which may have negative consequences in biological applications (James et al., 1998).

Patterning proteins using microcontact printing can result in either chemically or physically immobilized proteins. Printing of linking molecules (*e.g.* silanes) and pre-pattering the surface allows for further covalent coupling of the linking molecule with proteins and antibodies of

interest. This method has several benefits, including more durability and stability compared to physical immobilization in conditions such as under sheer stress. However, there are studies showing that during the stamping process, since the linking molecules (*e.g.* silanes) are relatively small, they can diffuse in and out of the PDMS stamp resulting in a low resolution (Didar et al., 2012; Sathish, Ricoult, Toda-Peters, & Shen, 2017). Direct microcontact printing of proteins and antibodies which leads to physical immobilization by hydrogen-bonding and van der Waals forces, may not be favourable in high sheer stresses conditions, but it is simple, fast, and has proven to be a promising method for numerous applications.

In chapter 3, we demonstrate that by microcontact printing anti-CD34 antibody on a glass substrate and by blocking the surface with our proposed blocking method explained in section 1.1.2.3, we are able to specifically capture cells on the patterned areas of the glass substrate.

1.1.2. Non-specific binding techniques

As mentioned in previous paragraphs, prevention of non-specific binding is a key element in biofunctional surfaces. There are several ways to implement this concept on a biofunctional surface. In this section, methods used in the literature for non-specific adhesion will be discussed.

1.1.2.1. Bovine serum albumin blocking

One popular method for preventing non-specific binding is surface treatments with bovine serum albumin (BSA) which is mostly referred to as a universal blocking agent. After immobilizing the protein or antibody of interest on the surface, BSA is incubated on the surface to block the undesirable sites on the surface. This allows only the immobilized antibody to bind with the target reagent, which might be an antibody or a specific cell (Andre Bernard et al., 1998; Camci-Unal et al., 2010; Jeyachandran, Mielczarski, Rai, & Mielczarski, 2009; MacBeath & Schreiber, 2000). Despite the wide use of BSA, some studies have shown that there is a weak attachment between

BSA and the surface, meaning it can be removed, due to physical adsorption of BSA on the surface (Falconnet, Csucs, Michelle Grandin, & Textor, 2006; Nelson, Raghavan, Tan, & Chen, 2003).

1.1.2.2. Ethylene Glycol

Poly- (ethylene glycol) (PEG) or oligo (ethylene glycol) (OEG) which are grafted on a given substrate or implemented into a polymer, are other methods for limiting non-specific binding of proteins to unwanted sites. Furthermore, PEG is also implemented on surfaces for prevention of platelet adhesion to blood contacting materials (Chen et al., 2012). The steric repulsion effect of PEG is responsible for repelling the proteins from the surface in such a way that it does not allow the proteins to reach the surface (Harder, Grunze, Dahint, Whitesides, & Laibinis, 1998). Although PEG based coating have been widely used, they have been proven not to be suitable for long-term applications and they are not durable (Gautrot et al., 2010). Also, alternative coatings, namely, omniphobic lubricant-infused surfaces, have proven to be a better choice for prevention of thrombosis (Badv et al., 2017).

1.1.2.3. Omniphobic lubricant-infused coating

A wide range of applications for surfaces that can repel various materials, such as inhibition of bacterial biofilm formation, fuel transport, or anti-ice formation in some industries, has led to increasing research in development of omniphobic surfaces. Nature often provides solutions to the problems we face, and pitcher plants inspired the development of an omniphobic liquid-infused surface (Wong et al., 2011). Pitcher plant's microtopography as well as hydrophilicity allows water to lock down on its surface, creating a smooth and slippery layer that does not allow insects to attach (Bauer & Federle, 2009). The pitcher plant-inspired surface is capable of repelling various materials, while also being pressure-stable, self-healing, stable, and durable (Wong et al., 2011). These surfaces consist of a lubricating liquid which is locked on a surface with micro/nano-porous

structures. The surfaces used for this application can have the porous characteristics themselves, such as Teflon nanofibrous membranes, or their porosity can be induced on the surface by chemical modification, generally by a fluorinated silane. Subsequently, the lubricant is immobilized on the roughened surface to generate the repellant surface which is due to the non-covalent affinity of the lubricant and the surface. In other words, the surface is wetted by the lubricant (**Figure 1.2**) (Aizenberg, Aizenberg, KANG, Wong, & Kim, 2015; Wong et al., 2011). The liquid repellency is characterized by the interfacial energy between the components of the system, which can be described by a low sliding angle (<5°) and a high contact angle (>100°) (Wong et al., 2011).

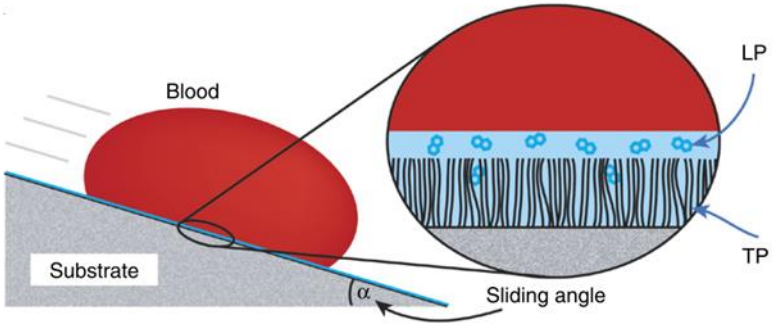

Figure 1.2. Schematic representation of a droplet of blood in contact with an omniphobic lubricant infused surface. TP is representative SAMs of fluorosilane and LP is representative of the lubricating liquid which has a stable and strong interaction with the TP layer. Adapted from (Leslie et al., 2014).

Chemical modification of the surface with a fluorinated silane is conducted by chemical vapor deposition (CVD) or liquid phase deposition (LPD) techniques, which each have their pros and cons (Badv et al., 2017). In CVD, the deposition of the desired film happens in a gaseous phase within a closed environment containing the substrate, whereas in LPD, the substrate is immersed in a liquid system, allowing the film to be deposited (Xu & Yan, 2010). In both CVD and LPD, the initial step is to induce hydroxyl groups on the surface either by oxygen plasma or by piranha solution. The Si molecule of the fluorinated silane, for example tridecafluoro-1,1,2,2-tetrahydrooctyl trichlorosilane, has four groups around it, one is the fluorinated tail and the rest

are chlorine groups. The general mechanism of the silanization reaction is that the chlorine molecules of the trichlorosilane part of the fluorinated silane and the OH groups of the surface take place in a direct nucleophilic displacement reaction, resulting in a monolayer of the fluorinated silane which is chemically anchored on the surface (Kleinfeld, Kahler, & Hockberger, 1988).

Examples of surfaces that have incorporated this bioinspired omniphobic liquid-infused approach are as follows:

- Anti-thrombogenic coating for blood contacting medical devices, such as catheters (Badv et al., 2017)
- Anti-ice and anti-frost performance for applications, such as refrigeration and aviation (P. Kim et al., 2012)
- Anti-biofouling and antibacterial performance for clinical and industrial applications (Epstein, Wong, Belisle, Boggs, & Aizenberg, 2012; Leslie et al., 2014; Li et al., 2013)
- High underwater transparency for controlling marine biofouling in optical instruments (Wang, Zhang, Sun, Li, & Sun, 2017)

1.2. Objectives and thesis outline

The main objectives of this work is to design and develop biofunctional lubricant-infused interfaces and demonstrate their application in controlled cell adhesion while preventing non-specific adhesion. Following are the detailed objectives:

- Tunable chemical immobilization of mixed organosilanes (aminosilanes and fluorosilanes) using liquid phase deposition (chapter 2)
- Tunable chemical immobilization of mixed organosilanes (aminosilanes and fluorosilanes) using chemical vapor deposition (chapter 2)

- Optimizing the mixed silanes to achieve simultaneous biofunctionality and omniphobicity (chapter 2)
- Demonstrating the biofunctionality of the developed omniphobic surfaces through controlled cell adhesion (chapter 2)
- Integrating microcontact printing and SAMs of fluorosilanes to develop patterned biofunctional omniphobic surfaces (chapter 3)
- Demonstrating cell patterning and controlled cell adhesion on micropatterned omniphobic surfaces (chapter 3)

1.3. References

Acres, R. G., Ellis, A. V., Alvino, J., Lenahan, C. E., Khodakov, D. A., Metha, G. F., & Andersson, G. G. (2012). Molecular structure of 3-aminopropyltriethoxysilane layers formed on silanol-terminated silicon surfaces. *Journal of Physical Chemistry C*, *116*(10), 6289–6297. https://doi.org/10.1021/jp212056s

Aizenberg, J., Aizenberg, M., KANG, S. H., Wong, T. S., & Kim, P. (2015). Slippery surfaces with high pressure stability, optical transparency, and self-healing characteristics. Google Patents. Retrieved from https://www.google.com/patents/US9121306

Awsiuk, K., Bernasik, A., Kitsara, M., Budkowski, A., Petrou, P., Kakabakos, S., … Raptis, I. (2012). Spectroscopic and microscopic characterization of biosensor surfaces with protein/amino-organosilane/silicon structure. *Colloids and Surfaces B: Biointerfaces*, *90*(1), 159–168. https://doi.org/10.1016/j.colsurfb.2011.10.017

Badv, M., Jaffer, I. H., Weitz, J. I., & Didar, T. F. (2017). An omniphobic lubricant-infused coating produced by chemical vapor deposition of hydrophobic organosilanes attenuates clotting on catheter surfaces. *Scientific Reports*, *7*(1), 11639. https://doi.org/10.1038/s41598-017-12149-1

Bauer, U., & Federle, W. (2009). The insect-trapping rim of Nepenthes pitchers: surface structure and function. *Plant Signaling & Behavior*, *4*(11), 1019–1023. https://doi.org/10.4161/psb.4.11.9664

Bernard, A., Delamarche, E., Schmid, H., Michel, B., Bosshard, H. R., & Biebuyck, H. (1998). Printing patterns of proteins. *Langmuir*, *14*(9), 2225–2229. https://doi.org/10.1021/la980037l

Bernard, A., Renault, J. P., Michel, B., Bosshard, H. R., & Delamarche, E. (2000). Microcontact printing of proteins. *Advanced Materials*, *12*(14), 1067–1070. https://doi.org/Doi 10.1002/1521-4095(200007)12:14<1067::Aid-Adma1067>3.0.Co;2-M

Camci-Unal, G., Aubin, H., Ahari, A. F., Bae, H., Nichol, J. W., & Khademhosseini, A. (2010). Surface-modified hyaluronic acid hydrogels to capture endothelial progenitor cells. *Soft Matter*, *6*(20), 5120–5126. https://doi.org/10.1039/c0sm00508h

Castner, D. G., & Ratner, B. D. (2002). *Biomedical surface science: Foundations to frontiers*. *Surface Science* (Vol. 500). https://doi.org/10.1016/S0039-6028(01)01587-4

Chen, J., Cao, J., Wang, J., Maitz, M. F., Guo, L., Zhao, Y., … Huang, N. (2012). Biofunctionalization of titanium with PEG and anti-CD34 for hemocompatibility and stimulated endothelialization. *Journal of Colloid and Interface Science*, *368*(1), 636–647. https://doi.org/10.1016/j.jcis.2011.11.039

Didar, T. F., Foudeh, A. M., & Tabrizian, M. (2012). Patterning multiplex protein microarrays in a single microfluidic channel. *Analytical Chemistry*, *84*(2), 1012–1018. https://doi.org/10.1021/ac2025877

Epstein, A. K., Wong, T.-S., Belisle, R. a, Boggs, E. M., & Aizenberg, J. (2012). Liquid-infused structured surfaces with exceptional anti-biofouling performance. *Proceedings of the*

National Academy of Sciences of the United States of America, *109*(33), 13182–13187. https://doi.org/10.1073/pnas.1201973109

Falconnet, D., Csucs, G., Michelle Grandin, H., & Textor, M. (2006). Surface engineering approaches to micropattern surfaces for cell-based assays. *Biomaterials*, *27*(16), 3044–3063. https://doi.org/10.1016/j.biomaterials.2005.12.024

Gautrot, J. E., Huck, W. T. S., Welch, M., & Ramstedt, M. (2010). Protein-resistant NTA-functionalized polymer brushes for selective and stable immobilization of histidine-tagged proteins. *ACS Applied Materials and Interfaces*, *2*(1), 193–202. https://doi.org/10.1021/am9006484

Gonzalez-Rodriguez, J., & Raveendran, M. (2015). Importance of Biosensors. *Biosensors Journal*, *4*(1), 4967. https://doi.org/10.4172/2090-4967.1000e104

Harder, P., Grunze, M., Dahint, R., Whitesides, G. M., & Laibinis, P. E. (1998). Molecular Conformation in Oligo(ethylene glycol)-Terminated Self-Assembled Monolayers on Gold and Silver Surfaces Determines Their Ability To Resist Protein Adsorption. *The Journal of Physical Chemistry B*, *102*(2), 426–436. https://doi.org/10.1021/jp972635z

James, C. D., Davis, R. C., Kam, L., Craighead, H. G., Isaacson, M., Turner, J. N., & Shain, W. (1998). Patterned Protein Layers on Solid Substrates by Thin Stamp Microcontact Printing. *Langmuir*, *14*(4), 741–744. https://doi.org/10.1021/la9710482

Jeyachandran, Y. L., Mielczarski, E., Rai, B., & Mielczarski, J. A. (2009). Quantitative and qualitative evaluation of adsorption/desorption of bovine serum albumin on hydrophilic and hydrophobic surfaces. *Langmuir*, *25*(19), 11614–11620. https://doi.org/10.1021/la901453a

Kasemo, B. (2002). Biological surface science. *Surface Science*, *500*(1–3), 656–677. https://doi.org/10.1016/S0039-6028(01)01809-X

Kim, D. J., Lee, J. M., Park, J. G., & Chung, B. G. (2011). A self-assembled monolayer-based micropatterned array for controlling cell adhesion and protein adsorption. *Biotechnology and Bioengineering*, *108*(5), 1194–1202. https://doi.org/10.1002/bit.23029

Kim, J., Cho, J., Seidler, P. M., Kurland, N. E., & Yadavalli, V. K. (2010). Investigations of chemical modifications of amino-terminated organic films on silicon substrates and controlled protein immobilization. *Langmuir*, *26*(4), 2599–2608. https://doi.org/10.1021/la904027p

Kim, P., Wong, T. S., Alvarenga, J., Kreder, M. J., Adorno-Martinez, W. E., & Aizenberg, J. (2012). Liquid-infused nanostructured surfaces with extreme anti-ice and anti-frost performance. *ACS Nano*, *6*(8), 6569–6577. https://doi.org/10.1021/nn302310q

Kleinfeld, D., Kahler, K. H., & Hockberger, P. E. (1988). Controlled outgrowth of dissociated neurons on patterned substrates. *The Journal of Neuroscience : The Official Journal of the Society for Neuroscience*, *8*(11), 4098–120. Retrieved from http://www.ncbi.nlm.nih.gov/pubmed/3054009

Kumar, A., & Whitesides, G. M. (1993). Features of gold having micrometer to centimeter dimensions can be formed through a combination of stamping with an elastomeric stamp and an alkanethiol "ink" followed by chemical etching. *Applied Physics Letters*, *63*(14),

2002–2004. https://doi.org/10.1063/1.110628

Leslie, D. C., Waterhouse, A., Berthet, J. B., Valentin, T. M., Watters, A. L., Jain, A., … Ingber, D. E. (2014). A bioinspired omniphobic surface coating on medical devices prevents thrombosis and biofouling. *Nature Biotechnology*, *32*(11), 1134–40. https://doi.org/10.1038/nbt.3020

Li, J., Kleintschek, T., Rieder, A., Cheng, Y., Baumbach, T., Obst, U., … Levkin, P. A. (2013). Hydrophobic liquid-infused porous polymer surfaces for antibacterial applications. *ACS Applied Materials and Interfaces*, *5*(14), 6704–6711. https://doi.org/10.1021/am401532z

Lin, Q., Ding, X., Qiu, F., Song, X., Fu, G., & Ji, J. (2010). In situ endothelialization of intravascular stents coated with an anti-CD34 antibody functionalized heparin-collagen multilayer. *Biomaterials*, *31*(14), 4017–4025. https://doi.org/10.1016/j.biomaterials.2010.01.092

Liu, Y., & Yu, J. (2016). Oriented immobilization of proteins on solid supports for use in biosensors and biochips: a review. *Microchimica Acta*, *183*(1), 1–19. https://doi.org/10.1007/s00604-015-1623-4

Lung, C. Y. K., & Matinlinna, J. P. (2012). Aspects of silane coupling agents and surface conditioning in dentistry: An overview. *Dental Materials*, *28*(5), 467–477. https://doi.org/10.1016/j.dental.2012.02.009

MacBeath, G., & Schreiber, S. L. (2000). Printing proteins as microarrays for high-throughput function determination. *Science*, *289*(September), 1760–1763. https://doi.org/10.1126/science.289.5485.1760

Mehrotra, P. (2016). Biosensors and their applications - A review. *Journal of Oral Biology and Craniofacial Research*, *6*(2), 153–159. https://doi.org/10.1016/j.jobcr.2015.12.002

Nelson, C. M., Raghavan, S., Tan, J. L., & Chen, C. S. (2003). Degradation of micropatterned surfaces by cell-dependent and -independent processes. *Langmuir*, *19*(5), 1493–1499. https://doi.org/10.1021/la026178b

Petersen, S., Strohbach, A., Busch, R., Felix, S. B., Schmitz, K. P., & Sternberg, K. (2014). Site-selective immobilization of anti-CD34 antibodies to poly(l -lactide) for endovascular implant surfaces. *Journal of Biomedical Materials Research - Part B Applied Biomaterials*, *102*(2), 345–355. https://doi.org/10.1002/jbm.b.33012

Plueddemann, E. P. (1991). Chemistry of silane coupling agents. In *Silane coupling agents* (pp. 31–54). Springer.

Rusmini, F., Zhong, Z., & Feijen, J. (2007). Protein immobilization strategies for protein biochips. *Biomacromolecules*, *8*(6), 1775–1789. https://doi.org/10.1021/bm061197b

Sathish, S., Ricoult, S. G., Toda-Peters, K., & Shen, A. Q. (2017). Microcontact printing with aminosilanes: creating biomolecule micro- and nanoarrays for multiplexed microfluidic bioassays. *The Analyst*, *142*(10), 1772–1781. https://doi.org/10.1039/C7AN00273D

Tan, A., Farhatnia, Y., de Mel, A., Rajadas, J., Alavijeh, M. S., & Seifalian, A. M. (2013). Inception to actualization: Next generation coronary stent coatings incorporating

nanotechnology. *Journal of Biotechnology*, *164*(1), 151–170. https://doi.org/10.1016/j.jbiotec.2013.01.020

Trilling, A. K., Beekwilder, J., & Zuilhof, H. (2013). Antibody orientation on biosensor surfaces: a minireview. *The Analyst*, *138*(6), 1619. https://doi.org/10.1039/c2an36787d

Turner, A. P. F. (2013). Biosensors: sense and sensibility. *Chemical Society Reviews*, *42*(8), 3184. https://doi.org/10.1039/c3cs35528d

Wang, P., Zhang, D., Sun, S., Li, T., & Sun, Y. (2017). Fabrication of Slippery Lubricant-Infused Porous Surface with High Underwater Transparency for the Control of Marine Biofouling. *ACS Applied Materials & Interfaces*, *9*(1), 972–982. https://doi.org/10.1021/acsami.6b09117

Wong, T.-S., Kang, S. H., Tang, S. K. Y., Smythe, E. J., Hatton, B. D., Grinthal, A., & Aizenberg, J. (2011). Bioinspired self-repairing slippery surfaces with pressure-stable omniphobicity. *Nature*, *477*(7365), 443–7. https://doi.org/10.1038/nature10447

Xu, Y., & Yan, X.-T. (2010). *Chemical Vapour Deposition*. London: Springer London. https://doi.org/10.1007/978-1-84882-894-0

Yazdani, S. K., Nakano, M., Otsuka, F., Kolodgie, F. D., & Virmani, R. (2012). Accelerating endothelialization of coronary stents by capturing circulating endothelial progenitor cells. *Interventional Cardiology*, *4*(2), 169–181. https://doi.org/10.2217/ica.11.99

Zhang, F., Sautter, K., Larsen, A. M., Findley, D. A., Davis, R. C., Samha, H., & Linford, M. R. (2010). Chemical vapor deposition of three aminosilanes on silicon dioxide: Surface characterization, stability, effects of silane concentration, and cyanine dye adsorption. *Langmuir*, *26*(18), 14648–14654. https://doi.org/10.1021/la102447y

Zhanga, S., Lin, Y., Altman, M., Lässle, M., Nugent, H., Frankel, F., … Rich, A. (1999). Biological surface engineering: A simple system for cell pattern formation. *Biomaterials*, *20*(13), 1213–1220. https://doi.org/10.1016/S0142-9612(99)00014-9

Chapter 2

Bio-interfaces with Simultaneous Repellency and Controlled Cell Adhesion

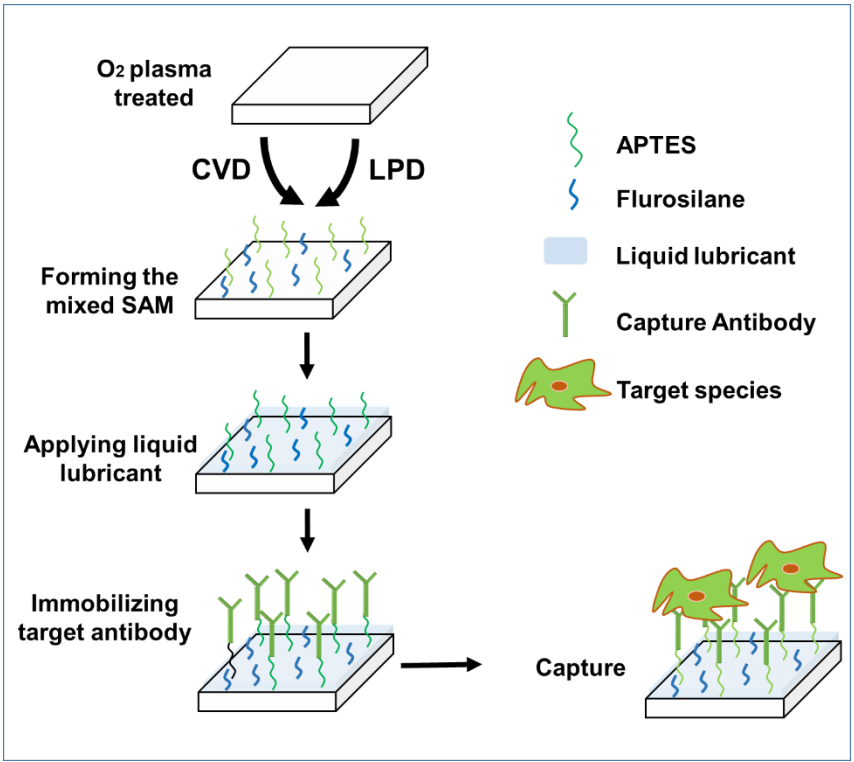

In chapter 2, all the experiments were conducted by myself and Maryam Badv who worked with me as a PhD student. My advisor, Prof. Didar gave me many helpful suggestions in both experiments and data analysis. Maryam Badv and I wrote the first draft of the paper. Prof. Didar, helped me in revising the draft to the final version.

Bio-interfaces with Simultaneous Repellency and Controlled Cell Adhesion

Sara M. Imani[1,Ψ], Maryam Badv[1,Ψ], Tohid F. Didar[1,2,3]

[1]School of Biomedical Engineering, McMaster University, Hamilton, Ontario, Canada.
[2]Department of Mechanical Engineering, McMaster University, Hamilton, Ontario, Canada.
[3]Institute for Infectious Disease Research (IIDR), McMaster University, Hamilton, Ontario, Canada

[Ψ]***These authors contributed equally to this work.***

Correspondence author:

Tohid F. Didar, PhD

Department of Mechanical Engineering and School of Biomedical Engineering, McMaster University

1280 Main Street West, JHE-308A, Hamilton, Ontario, Canada, L8S 4L7

ph: +1-905-5259140 Ex. 20413, fax: +1-905-572-7944

Email: didar@mcmaster.ca

Abstract

Development of biofunctional surfaces which prevent non-specific adhesion, has been subject of intensive research. Liquid-infused omniphobic coatings which are based on producing self-assembled monolayers (SAMs) of fluorosilanes, have been proven to be robust and durable coatings that can prevent biofouling and thrombin generation. In this study, we report that producing different ratios of mixed SAMs of fluorosilanes along with aminosilanes, will lead to further developing tunable biofunctional liquid-infused omniphobic coatings. Mixed SAMs of these organosilanes were integrated onto the surface using chemical vapor deposition (CVD) and liquid phase deposition (LPD). Furthermore, via EDC-NHS chemistry biomolecules of interest, in this case anti-CD34 antibodies, were immobilized through amine groups on the aminosilanes. In presence of our proposed blocking method, we were able to control the degree of which the

biomolecules were attached to the surface. To evaluate the biofunctionality and its controllability, samples were incubated with red fluorescent protein expressing human umbilical vein endothelial cells (RFP-HUVEC). Herein we demonstrated that we were able to control cells' adherence to the surface by changing the ratio of the mixed SAMs of the organosilanes and further evaluated the cytotoxicity of the treated surfaces by MTT assay which confirmed that our proposed coating is not toxic for the cells.

1. Introduction

Advancement of efficient smart biofunctional surfaces has been the subject of intensive research for the past decade due to their numerous applications in bioengineering including biosensors, medical implants, and medical diagnostics and therapeutics (Castner & Ratner, 2002). Optimum performance for surfaces which biomolecules are immobilized on, requires targeted binding and prevention of non-specific adhesion or non-fouling surface characteristics (Gautrot, Huck, Welch, & Ramstedt, 2010; Rusmini, Zhong, & Feijen, 2007). For instance, in case of medical implants, lack of biofunctionality and presence of non-specific adhesion, would result in delayed healing, thrombosis, and biofilm formation (Camci-Unal et al., 2010; Jialong Chen et al., 2012; Yin, Yuan, Liu, & Wang, 2009). Therefore, increasing smart bio-compatibility through integration of non-fouling surfaces while maintaining targeted functionality is vital. Moreover, in addition to producing an irreversible and stable protein binding to the surface, sensitivity of the biosensors relies on reducing background signal which is a result of non-specific binding of biomolecules (J. Kim, Cho, Seidler, Kurland, & Yadavalli, 2010; Y. Liu & Yu, 2016).

Development of modified surfaces for targeted binding using self-assembled monolayers (SAMs) of silanes, is one of the widely used methods for covalent attachment of organic and inorganic materials (Lung & Matinlinna, 2012). This capacity of silane coupling agents, makes them a

promising candidate for producing biofunctional surfaces. 3-aminopropyltriethoxy-silane (APTES) is one of the most extensively used molecules of such silanes (Awsiuk et al., 2012, 2013; Filippini et al., 2001; Jang & Liu, 2009; D. J. Kim, Lee, Park, & Chung, 2011; J. Kim et al., 2010) and glass is often utilized to investigate the biofunctional properties added by silanization (Acres et al., 2012; Truskey & Proulx, 1993). The ethoxy terminal of APTES is responsible for the self-assembly through Si-O-Si bonds with the hydroxylated glass surface (Acres et al., 2012; W. Wang & Vaughn, 2008) while the amine (NH_2) terminal allows for covalent bonding of biomolecules (Awsiuk et al., 2013).

In addition to biofunctionality, one of the key characteristics of a biofunctional surface is to have reduced non-specific binding of biomolecules (Castner & Ratner, 2002) and many strategies have been developed to overcome this limitation. Surface treatments with bovine serum albumin (BSA) (Camci-Unal et al., 2010; Jialong Chen et al., 2012; Didar, Foudeh, & Tabrizian, 2012; Li et al., 2010; Qin et al., 2007) has been widely used to saturate the unoccupied regions when a surface had been previously treated with biomolecules (Jeyachandran, Mielczarski, Rai, & Mielczarski, 2009). However, BSA cannot prevent blood coagulation and biofilm formation and since the immobilization of BSA is done physically, there is a weak attachment between BSA and the surface and that can be easily broken (Rusmini et al., 2007). Poly-(ethylene glycol) (PEG) (Anderson et al., 2008; Jialong Chen et al., 2012; Tsai, Chen, & Chien, 2009) is also used for limiting nonspecific protein adsorption. However, PEG has some drawbacks such as durability and stability for long-term applications (Gautrot et al., 2010). More recently, the wide range of potential applications for omniphobic surfaces has led to intense research in development of such surfaces. Lubricant-infused surfaces are among the most recent omniphobic coatings that have demonstrated successful icephobicity (P. Kim et al., 2012), anti-biofouling performance (Epstein,

Wong, Belisle, Boggs, & Aizenberg, 2012; P. Wang, Zhang, Sun, Li, & Sun, 2017), and anti-thrombogenic characteristics (Badv, Jaffer, Weitz, & Didar, 2017; Leslie et al., 2014). These surfaces are produced by fabricating self-assembled monolayers of fluorosilanes (*e.g.* trichloro (1H,1H,2H,2H-perfluorooctyl) silane (TPFS)) on a desired surface followed by infusing a biocompatible perfluorocarbon lubricating liquid (*e.g.* perfluoroperhydrophenanthrene (PFPP)) which creates a strong and stable interaction between the fluorinated silane and the lubricant (Leslie et al., 2014; Wong et al., 2011) and has been proven to be robust and highly stable (Wong et al., 2011).

Omniphobic lubricant-infused surfaces and biofunctionality appear to be mutually exclusive characteristics, since an omniphobic lubricant-infused surface intends to produce properties preventing biomolecules from interacting with the surface, while biofunctionality enhances target species capture on the surface and integration of these two properties has not been possible so far. In this study, we propose a novel technique that generates an omniphobic lubricant-infused biofunctional surface by producing mixed SAMs of APTES and TPFS in which APTES is used to covalently immobilize biomolecules via EDC-NHS chemistry and TPFS with the PFPP lubricant on the surface resulting in simultaneous targeted binding and repellency. Varying the ratios of APTES and TPFS in the reaction, followed by addition of PFPP, leads to creation of a platform for a tunable non-fouling biofunctional surface. Chemical modification of the surface with the silanes can be achieved by chemical vapor deposition (CVD) and Liquid-phase deposition (LPD) (Jönsson, Olofsson, Malmqvist, & Rönnberg, 1985). The general consensus for such reactions is an initial hydroxylation of glass and, subsequently, silanization between APTES and TPFS, and the surface.

We optimized creating mixed SAMs using both LPD and CVD methods and determined the omniphobicity of the surfaces by measuring the contact and sliding angles of the modified surfaces. Furthermore, biofunctionality of the samples which had different ratios of APTES and TPFS were investigated by an *in vitro* endothelialisation assay in order to examine the proper ratio for the silanes. In the assay, fluorescently labelled mouse anti-human CD34 monoclonal antibodies were immobilized on the lubricant-infused samples by activation of APTES through EDC-NHS chemistry, forming a covalent attachment between anti-CD34 antibody and APTES. Following this, samples were incubated with red fluorescent protein expressing human umbilical vein endothelial cells (RFP-HUVEC), allowing the anti-CD34 coated surface to capture RFP-HUVECs as anti-CD34 antibody is naturally present on the cell's surface, resulting in a tunable biofunctional platform which omniphobic lubricant-infused surfaces were used as a blocking method. We demonstrated control over the degree of cell adhesion by varying the mixed SAMs ratio. In addition, our results showed that the 75% ratio of APTES to TPFS provided the best condition to achieve both biofunctionality and omniphobicity.

2. Materials and Methods

2.1. Materials

Trichloro (1H,1H,2H,2H-perfluorooctyl) silane (TPFS), 3-aminopropyltriethoxy-silane (APTES), Phosphate Buffered Saline (PBS), Bovine Serum Albumin (BSA), perfluoroperhydrophenanthrene (PFPP), N-(3-Dimethylaminopropyl)-N′-ethylcarbodiimide (EDC), N-Hydroxysuccinimide (NHS) and 2-(N-Morpholino)ethanesulfonic acid (MES) were purchased from Sigma–Aldrich (Oakville, Canada). Red Fluorescent Protein Expressing Human Umbilical Vein Endothelial Cells (RFP-HUVEC) were generously provided by Dr. P. Ravi Selvaganapathy's lab at McMaster University. Cell media kit (EGM-2 BelletKit) and Trypsin neutralizing agent where purchased

from Cedarlane (Burlington, Canada). Trypsin-EDTA (0.25%), phenol red and the MTT cell proliferation assay kit was purchased from Thermo Fisher Scientific (Waltham, United States). Plain vista vision microscope slides were purchased from VWR (Radnor, United States).

2.2. Initial activation of the surfaces using oxygen plasma treatment

Plain microscope glass slides were used as main substrates throughout the experiments. Prior to starting the surface modification process, glass slides were cut in to small squares (about 0.5x0.5 cm^2) using a carbide handheld glasscutter, washed with 100% ethanol, sonicated for 10 minutes and dried under nitrogen flow. Glass substrates were then put in a plastic petri dishes, placed in an oxygen plasma cleaner (Harrick Plasma Cleaner, PDC-002, 230V) and exposed to high-pressure oxygen plasma for 5 minutes to functionalize their surfaces with hydroxyl groups (OH).

2.3. Producing mixed SAMs of silanes using Chemical Vapor Deposition (CVD)

After removing the oxygen plasma-treated glass slides from the plasma cleaner, they were placed in a desiccator and droplets of TPFS and/or APTES were added in a separate petri dish, reaching a total volume of 200 µL and placed beside the glass samples. After adding the proper amount of the silanes, the vacuum pump was turned on and the outlet valve of the desiccator was closed once a pressure of −0.08 MPa was reached in order to start the CVD process. In order to optimize the ratio between the amino and fluorosilane, different ratios of TPFS and APTES were added during the modification process. Samples with three different ratios of 95%-APTES 5%-TPFS, 75%-APTES 25%-TPFS, and 50%-APTES 50%-TPFS were prepared and samples containing 100% APTES or 100% TPFS were prepared and used as controls. The silanization reaction was carried out for 2 hours at room temperature. After the CVD step, glass slides were removed from the desiccator and placed in an oven at 60 ºC for a minimum of 12 hours in order to complete the reaction. Further, in order to insure the removal of non-covalently attached silane molecules from

the glass surfaces, they were sonicated for 10 minutes and subsequently placed in a vacuum desiccator for 30 mins.

2.4. Producing mixed SAMs of silanes using Liquid Phase Deposition (LPD)

Glass slides were oxygen plasma treated as described above and then immediately incubated in a 50 mL plastic tube containing TPFS and/or APTES in anhydrous ethanol solution (5% v/v). Similar to the CVD modification method, three different ratios of the amino and fluorosilane were prepared and samples made with 100% APTES or 100% TPFS were used as controls. The silane solutions containing the glass samples were stirred for 1 hour at room temperature and then the glass samples were removed from the solution, washed with 100% anhydrous ethanol and deionized water and ultimately 70% ethanol was used to complete the washing step. After drying the samples at room temperature, they were placed in the oven at 60ºC overnight for at least 12 hours. Similar to CVD treated samples, after removing the LPD treated glass slides from the oven, they were sonicated for 10 minutes and placed under vacuum for 30 mins so that the non-covalently attached silane molecules will be removed.

2.5. Characterization of the SAM

2.5.1. XPS

X-ray photo electron spectroscopy (XPS) was used to measure the surface chemical composition of the treated glass samples after CVD and LPD treatment. Three glass segments were submitted for each condition and means were determined. A Physical Electronics (PHI) Quantera II spectrometer equipped with an Al anode source for X-ray generation was used to record the XPS spectra (BioInterface Institute, McMaster University). XPS results were obtained at 45˚ take off angles with a pass energy of 280 eV. The atomic percentages of carbon, oxygen, fluorine and silicon was calculated using the instrument's software.

2.5.2. Fluorescein isothiocyanate (FITC) labeling

In addition to XPS measurements, samples modified with the mixed silanes were further incubated with fluorescein isothiocyanate isomer I which is an amine targeting dye, in order to investigate the presence of APTES on the treated surfaces. A solution of 0.001 mg/mL FITC in carbonated buffer was prepared and 300 µL of the solution was added to the glass slides. Prior to adding the FITC solution on the glass samples, lubricant was added on samples that were prepared with both the TPFS and APTES in order to prevent physical adhesion of the FITC to the hydrophobic regions on the surface. Glass samples were incubated with the FITC solution overnight and they were washed with PBS and water after the incubation period. Samples were imaged using fluorescent microscope and the fluorescence intensity was then measured using ImageJ software.

2.5.3. Atomic Force Microscopy (AFM)

The morphology and roughness of the silanized surfaces was evaluated by AFM (BioScope Catalyst, Bruker). All measurements were performed in ScanAsyst mode. A probe with spring constant of 0.4 N/m was used to obtain a scan size of 1 × 1 µm of each of the glass substrates.

2.6. Characterization of the omniphobic slippery properties – Contact and Sliding angle measurements

In order to investigate the omniphobic slippery properties of the modified and control samples, their contact and sliding angles were measures using a 5 µL droplet of deionized water. Water sessile drop contact angle measurements were performed at room temperature after modifying the glass slides with silane molecules, using a Future Digital Scientific OCA20 goniometer (Garden City, NY). The contact angle goniometer was calibrated prior to each measurement.

Sliding angles were measured using a digital angle level (ROK, Exeter, UK). Prior to starting the measurements, silanized samples coated with PFPP were placed on the calibrated level and a 5µL

droplet of deionized water was placed on the glass surface. The level was gently angled until the droplet would start to move on the glass slide and the sliding angle was defined as the minimum angle required for droplets to start sliding on the glass substrate. For samples that the droplet failed to slide at angles of 90 degrees or higher, a sliding angle of 90 degrees was assigned. Measurements were performed on three different glass segments and means were determined.

2.7. Biofunctionality

2.7.1. Surface functionalization using anti-CD34 antibody

In order to make the silane modified surfaces biofunctional, treated samples were functionalized with the anti-CD34 antibody using the carbodiimide crosslinker chemistry. Anti-CD34 antibody solution with a concentration of 1 µg/mL in 0.1 M MES buffer (pH 5.5) was prepared and activation was initiated by adding EDC and NHS to the solution yielding to 2 mM EDC and 5 mM NHS respectively. Treated glass samples were placed inside the wells of a 48 well plate and all samples that were modified with both APTES and TPFS were saturated with PFPP lubricant prior to adding the antibody in order to minimize the non-specific binding (**Figure 2.1**). After removing the excess lubricant, each sample was incubated with 300 µL of the anti-CD34 solution for 2 hours at room temperature and later on incubated at 4 °C overnight. Samples were washed with PBS and DI water in order to remove the non-covalently attached antibodies. All anti-body experiments were performed in the Biosafety Cabinet (BSC) and samples were kept sterile.

2.7.2. Cell adhesion and cell growth

After modifying the glass surfaces with anti-CD34 antibody, their biofunctionality and repellency properties were evaluated by looking at cell growth and cell attachment on their surfaces (**Figure 2.1**). Glass substrates that were placed in 48 well plates were incubated with 300 µL of RFP-HUVECs in cell media with a density of 1.5 x 10^5 cells/mL. RFP-HUVECs of passage 4-6 were

used for cell studies. Cell containing plates were placed in a 5% CO_2 incubator at 37 °C and samples were taken out after 6 and 48 hours incubation time, washed and imaged using a fluorescence microscope. The potency of each surface for cell attachment and cell repellency was evaluated by counting the number of cells attached to the surface. Surfaces blocked using BSA or TPFS with no lubricant were also investigated as controls and the results obtained from these surfaces were compared with other treated surfaces.

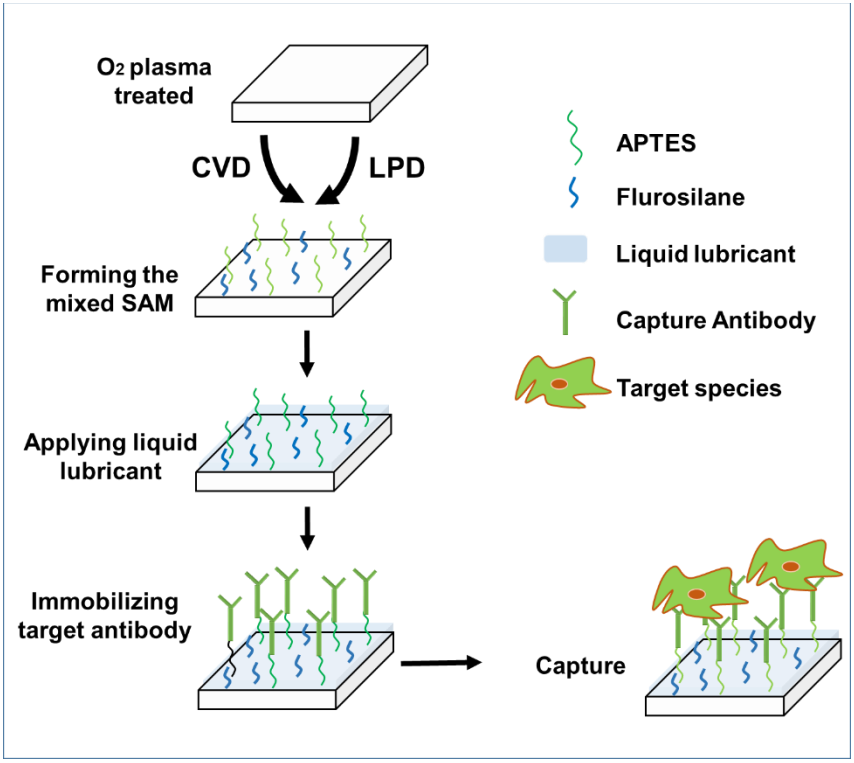

Figure 2.1. Schematic representation of creating omniphobic lubricant infused biofunctional surfaces using chemical vapor deposition (CVD) and liquid phase deposition (LPD) of mixed SAMs of amino and fluorosilanes. The oxygen plasma treated glass slides were treated with different ratios of APTES or TPFS using the CVD or LPD methods. After treating the samples, liquid lubricant was added to create the omniphobic slippery surfaces and further on, the anti-CD34 antibody was attached to the surface using the EDC-NHS chemistry. In the next step, HUVECs where seeded on the samples to investigate the degree of cell adhesion.

2.8. *In vitro* cytotoxicity against RFP-HUVECs – MTT assay

In order to investigate the cytotoxicity of the treated surfaces, MTT assay was performed. Briefly, RFP-HUVECs were grown in cell media and seeded with a density of 1.5 x 10^4 cells/mL in a 48

well plate. After 6 and 48 hours of culture, 300 µL fresh media and 30 µL of 12 mM MTT solution was added to each well and the well plate was incubated for an additional 4 hours at 37 °C. Subsequently, 150 µL DMSO was added to 75 µL of each well to dissolve the dark blue crystals. Absorbance was measured at 570 nm wavelength on a SpectraMax plate reader. All measurements were repeated in triplicate.

2.9. Statistical Analysis

All data are presented as means ± S.D. Each experiment condition was repeated at least three times. To access statistical significance between different groups, one-way analysis of variance (ANOVA) followed by post hoc analysis using Tukey's test was performed. P values less than 0.05 were considered statistically significant for all comparisons.

3. Results and Discussion

3.1. Presence of TPFS and APTES on the treated surfaces

3.1.1. XPS analysis for Fluorine – presence of TPFS

XPS was performed to investigate the presence of the TPFS molecule on the glass surfaces treated with different ratios of APTES to TPFS by measuring the Florine atom % of the coated glass slides after the CVD or LPD treatment methods (**Figure 2.2a**). The Fluorine atom % on each sample treated with different ratios of APTES to TPFS was measured and the results from each treatment group was compared with each other. In the CVD treated samples, there was a descending trend between the atom % of Fluorine and the volume % of TPFS used in the modification process. Samples treated with 100% TPFS (0% APTES) had the highest atom % of Fluorine (51.9 ± 3.4 atom %), and the atom % of Fluorine decreased by decreasing the volume % of TPFS used, with samples treated with 5% TPFS (95% APTES) having the lowest amount of Fluorine (12.3 ± 9.5 atom %) compared to other ratios. In contrast to CVD treated samples, when comparing the results

obtained from LPD treated experiments, there was no defined relationship between the atom % Fluorine and the different silane ratios. In the LPD treatment group, samples treated with 95% TPFS had the highest amount of Fluorine (53.1 ± 0.6 %) and there was no significant difference between the Fluorine atom % when comparing the results from other ratios (100% TPFS, 50% TPFS and 25% TPFS). When comparing the results of different ratios obtained from the two CVD or LPD treatment methods, CVD treated samples had a higher amount of Fluorine compared to LPD treated samples, although the differences were not significant.

These results show that the amount of TPFS on the surface could be controlled by tuning the ratio of APTES to TPFS used in the modification step in the CVD processing method. However, controlling the silane deposition on the surface is more challenging when using the LPD method. Previous studies have also shown that CVD is more effective and reproducible than LPD in generating homogenous silanized layers (Badv et al., 2017; Zhang et al., 2010).

3.1.2. Fluorescence staining of amine groups – Presence of APTES

The amount of APTES present on the glass surfaces treated with the CVD or LPD technique was quantified by fluorescence imaging after labelling the surfaces with a fluorescently labelled amine targeting molecule (**Figure 2.2b**). Images were taken from the treated surfaces and the amount of green fluorescence intensity was calculated using ImageJ. In the CVD treated group, samples modified with 100% APTES (0% TPFS) had the highest amount of fluorescence intensity compared to other groups (91.7 ± 13.9 a.u.). As the ratio of the APTES used decreased, the fluorescence intensity also decreased and samples with no APTES (100% TPFS) had the lowest amount of amine groups on their surfaces (3.1 ± 2.7 a.u.). Similar to the results obtained from the XPS measurements of the Fluorine element, the amine staining results obtained from the CVD experiments also confirm the homogeneity of the APTES layer created on the surface.

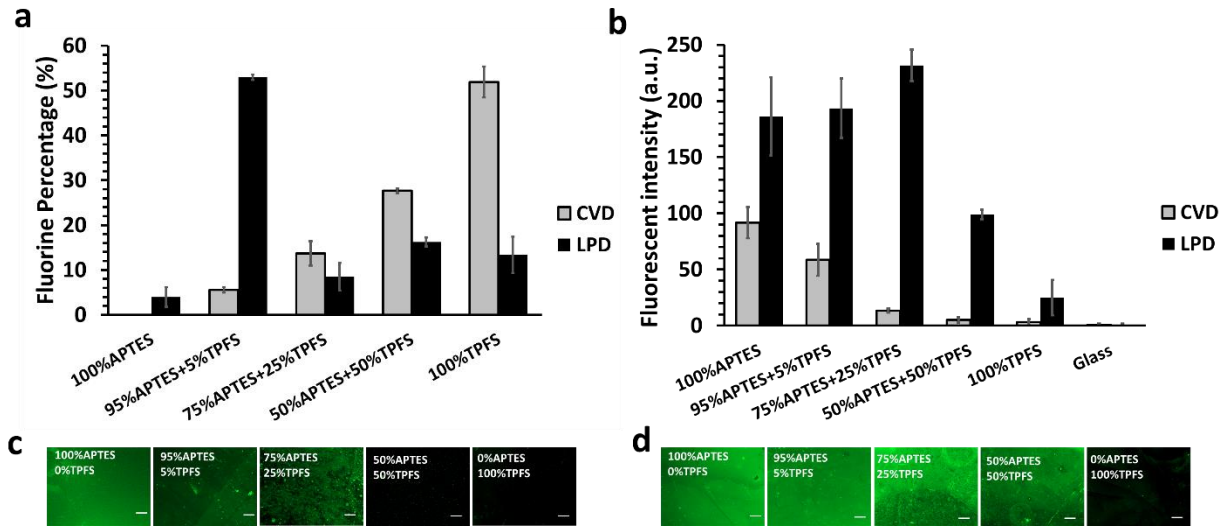

Figure 2.2. The chemical composition of the treated surfaces determined by a) XPS and b) amine labeling. a) XPS analysis in order to determine the presence of TPFS (Florine atom percentage) after surface modification. **b)** Samples were functionalized with Fluorescein isothiocyanate isomer I (FITC) which is an amine targeting dye and the fluorescent intensity was calculated. **c** and **d)** Representative fluorescent images with 10X magnification of FITC functionalized surfaces are shown for CVD and LPD respectively (Scale bar: 100 μm).

In contrast to CVD treated samples, in LPD treated samples, the FITC intensity did not follow a defined trend and samples treated with 75% APTES had the highest amount of FITC (231.7 ± 14.1 a.u.), followed by 95% APTES and 100% APTES (193.6 ± 26.6 a.u. and 186.4 ± 34.9 a.u. respectively). The differences between these ratios were not significant. Similar to the CVD treated samples, samples treated with 0% APTES (100% TPFS) had the lowest amount of amine groups on their surface. In general, when comparing the results from the two different treatment methods, LPD treated samples had a significantly higher amount of amine groups on their surfaces compared to CVD treated samples. This was in-line with the XPS results obtained for the Fluorine element. Since LPD treated samples had a lower amount of TPFS on their surfaces, it could be expected to see a higher amount of APTES (higher fluorescence intensity of FITC) on these surfaces compared to the CVD treated samples. The fluctuation seen in the FITC intensity of the LPD treated samples, and not in the CVD treated samples, confirms the heterogeneous deposition of the APTES

molecule from the liquid phase, again suggesting that the CVD method is a more reliable technique for creating homogenous silane layers (Z. Z. Liu, Wang, Liu, & Bao, 2008; Zhang et al., 2010).

3.2. Sliding and contact angle measurements

Further on, in order to evaluate the omniphobic slippery properties of the treated samples, sliding and contact angle measurements were performed using a 5 µL droplet of deionized water (**Figure 2.3**). The sliding angle was defined as the minimum tilting angle required for the droplet to start moving on the glass substrate. A sliding angle of 90 degrees was assigned to samples that the droplets would fail to slide at angles of 90 degrees or higher. Both CVD and LPD samples treated with a mixed ratio of APTES and TPFS had sliding angles as low as 5 ° (**Figure 2.3a**). The droplets did not slide on samples that were treated with 100% APTES (0% TPFS), plain glass slides and glass slides that were plasma treated only.

The static contact angle measurements of the control and treated glass surfaces before adding the lubricant layer are shown in **Figures 2.3b.** Samples that were treated with 100% APTES, in the CVD group were hydrophilic and their average static contact angle was below 90 ° (θ_{st} = 86.91 ± 2.27). In contrast to CVD treated samples, the 100% APTES, LPD treated samples were slightly hydrophobic (θ_{st} = 93.92 ± 3.74). In both CVD and LPD treated groups, samples that were treated with a mixed ratio of APTES and TPFS showed hydrophobic properties by revealing an average static contact angle above 100 °. In both CVD and LPD treated samples no significant difference was observed in the contact angle measurement when comparing the results obtained from 100% TPFS treated samples with those treated with both APTES and TPFS.

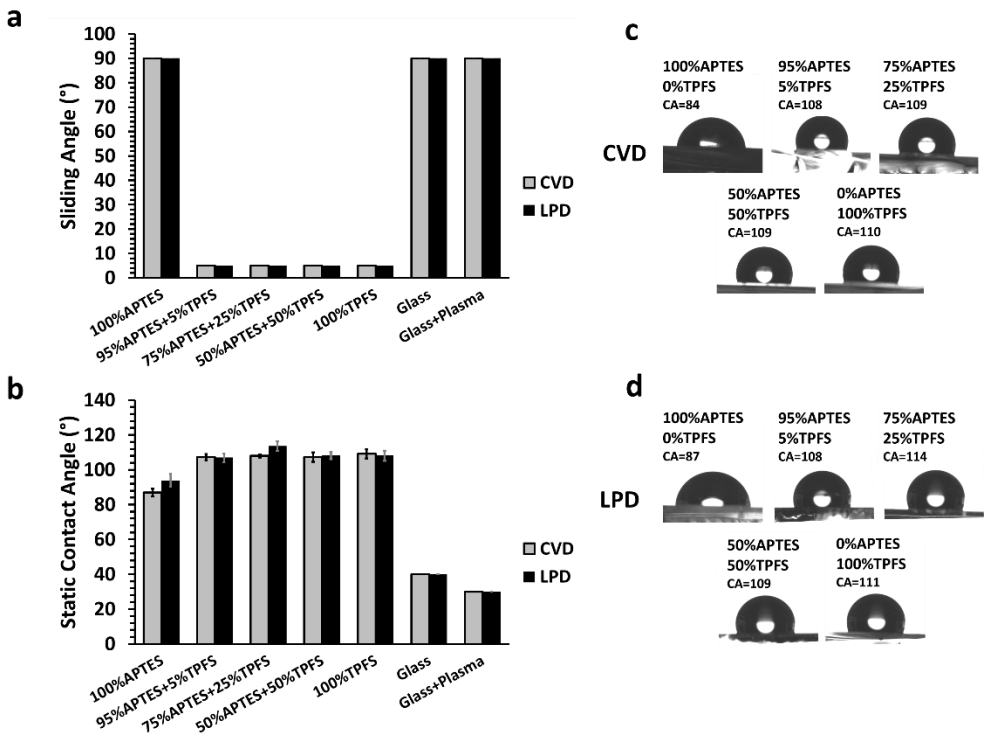

Figure 2.3. Sliding and contact angle measurements of treated samples and controls. a) CVD and LPD silane treated samples were lubricated and a 5 uL droplet was placed on the surface of the samples and the sliding angle was measured by lifting the surface and recording the angle which the droplet starts to move. **b)** Static Contact angle measurements of the surfaces were measured prior to lubricating the surfaces (The results are presented as means ± SD). **c** and **d)** Representative contact angle images of a 5 µL water droplet on the surfaces are shown for CVD and LPD respectively.

Results obtained from the sliding and contact angle measurements confirm that all APTES to TPFS surfaces treated with mixed SAMs using CVD or LPD method have excellent omniphobic slippery properties and the presence of a minimum amount of TPFS (as low as 5 volume %) is sufficient to obtain omniphobic slippery properties. The results for contact and sliding angle measurements in samples prepared with a mixture of APTES and TPFS are comparable to previous studies that created omniphobic slippery properties using 100% TPFS only (Badv et al., 2017; Leslie et al., 2014; Wong et al., 2011).

3.3. Surface topography and roughness

The surface topography and roughness of the produced mixed SAMs was investigated using AFM. **Figure 2.4a** shows the surface topography and roughness values for silanized samples from both CVD and LPD treated groups. All measurements were carried out in the ScanAssist mode. Overall, both LPD and CVD modification techniques created a relatively smooth layer. Samples treated 95% APTES (5% TPFS) had the highest RMS roughness of 7.38 ± 0.01 nm. When comparing the CVD and LPD treated samples with 100% TPFS, CVD treated samples created a significantly smoother layer compared to LPD samples (0.67 ± 0.09 nm and 3.25 ± 0.23 nm respectively). The RMS roughness value of the 100% TPFS surfaces modified using the CVD method was comparable to the roughness of the non-modified glass slide (0.50 ± 0.01 nm). In the 100% APTES treated samples, the CVD method resulted in a smoother layer compared to the LPD treated method as well, with CVD samples having an average RMS roughness value of 2.71 ± 0.64 nm compared to 4.54 ± 0.68 nm in the LPD treated samples.

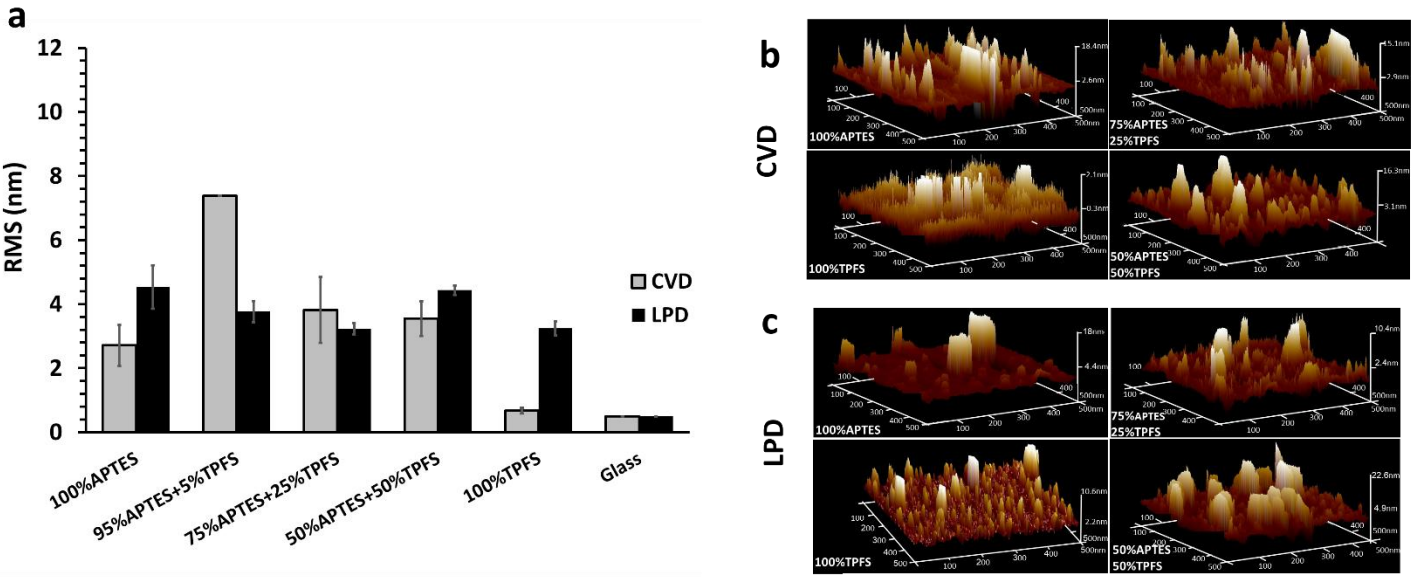

Figure 2.4. AFM results of the mixed silane treated surfaces. a) RMS measurements. Treated surfaces were subjected to AFM measurements in order to look at the surfaces morphology and roughness of the silane layer formed on the surface. **b** and **c)** Representative AFM 3D images of the surfaces are shown for CVD and LPD respectively.

3.4. Anti-CD34 antibody immobilization

The omniphobic slippery surfaces were biofunctionalized by attaching mouse anti-human anti-CD34 to the amine group present on their surfaces using the EDC-NHS chemistry. These antibodies were further on used as cell receptors for specific capture of RFP-HUVECs. The anti-CD34 antibody was fluorescently labeled with Alexa Fluor 488 and similar to FITC labelling, this fluorophore was used to quantify the amount of antibody attached on the surface using fluorescence microscopy. As seen in **Figure 2.5a**, in the CVD treated samples, similar to the results obtained from the FITC experiments, a linear correlation was seen between the percentage of APTES used in the modification step and the amount of CD34 attached to the surface. Samples treated with 100% APTES (0% TPFS) had the highest amount of the anit-CD34 antibody (78.74 ± 9.42 a.u.) followed by 95% APTES (5% TPFS) and 75% APTES (25% TPFS) samples with 53.35 ± 14.45 a.u. and 36.89 ± 16.53 a.u. respectively. The fluorescence intensity obtained from samples treated with 50% APTES (50% TPFS) suggested that these samples had a significantly lower amount of anti-CD34 antibody attached to their surface (0.91 ± 0.47 a.u.) and the fluorescence intensity obtained from these samples was similar to 100% TPFS (0% APTES) treated samples. The antibody immobilization experiments using CVD further confirmed the controllability and reliability of the silanized layer obtained using this technique (Zhang et al., 2010).

In contrast to CVD treated samples, no significant difference was seen in the fluorescence intensity between the samples from different treatment ratios in the LPD modified surfaces. Samples treated with 100% APTES (0% TPFS), 95% APTES (5% TPFS) and 75% APTES (25% TPFS) had similar amounts of anti-CD34 antibody attached to their surfaces (88.27 ± 7.26, 87.05 ± 15.41 and 76.78 ± 9.34 a.u. respectively) and no significant difference was seen between these samples.

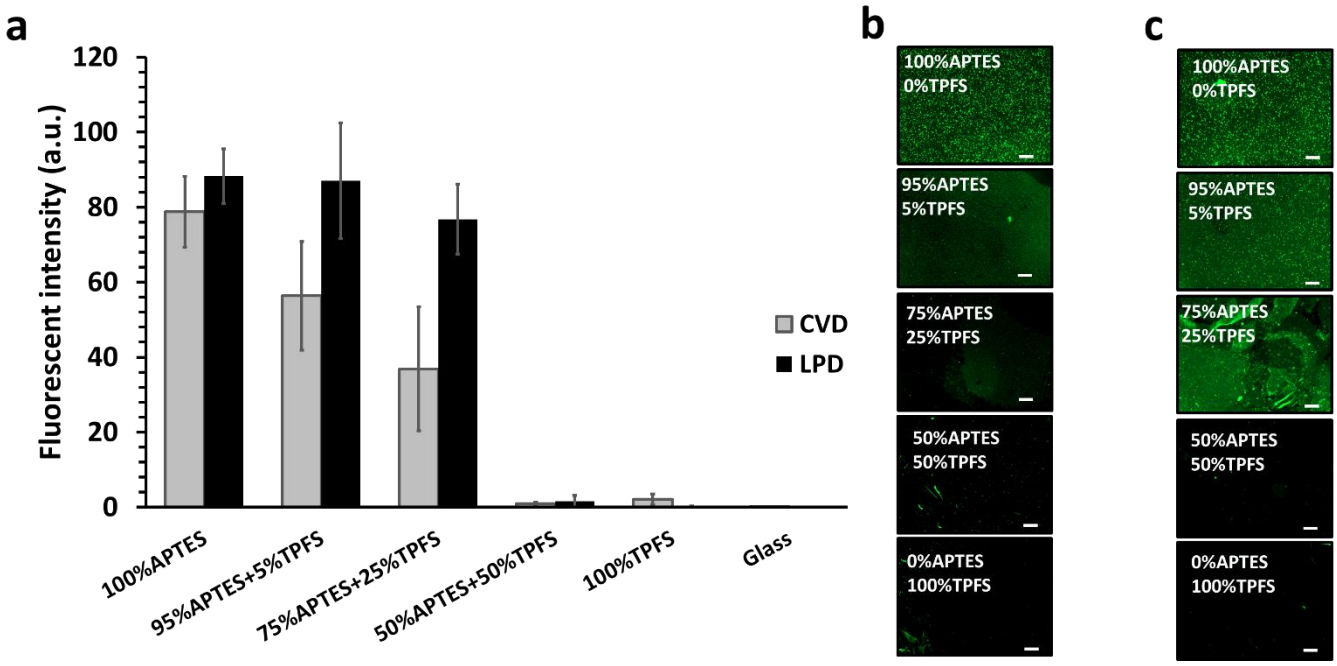

Figure 2.5. Anti-CD34 immobilization on the treated samples and controls. CVD and LPD silane treated samples were functionalized with anti-CD34 antibody. **a)** Fluorescent intensity of CD34 treated samples. Samples treated with 100% APTES had the highest intensity and samples that had no APTES, had significantly lower CD34 attachment. **b** and **c)** Representative fluorescent images with 10X magnification of anti-CD34 functionalized surfaces are shown for CVD and LPD respectively (Scale bar: 100 μm).

Similar to the results obtained from the 50% APTES treated samples in the CVD method, 50% APTES treated samples in LPD had significantly lower amounts of anti-CD34 antibody attached to their surface (1.57 ± 1.55 a.u.). This phenomena seen in both CVD and LPD treated samples could be due to the high percentage of TPFS present on the surface in the 50 % APTES (50% TPFS) samples. Fluorinated molecules such as TPFS are hydrophobic and have protein and cell repellency properties (Spargo et al., 1994). The high percentage of TPFS present on the 50 % APTES (50% TPFS) surfaces could cause a competition between these two molecules, dividing the modified surface into two regions of protein repellent and protein friendly. Results obtained from these experiments confirm the higher probability of these surfaces to act as protein repellent surfaces and as a result decreasing the chemical functionality of the APTES molecule. In addition, the density of the available functional groups on the surface for protein adhesion plays an important

role (Arima & Iwata, 2007). Results obtained from the 50% APTES (50% TPFS) treated surfaces show that the density of the APTES amine groups compared to the repellent TPFS regions might not be sufficient enough to immobilize the anti-CD34 antibodies on the surface.

When comparing the results obtained from the CVD treatment method with those from the LPD treatment method, LPD treated samples had a higher amount of anti-CD34 antibody immobilization, which was in-line with the results obtained from the FITC experiments.

3.5. Controlled cell attachment and surface cell repellency properties

The biofunctionality of the dual biofunctional omniphobic slippery surfaces was evaluated by incubating RFP-HUVECs with the anti-CD34 antibody functionalized surfaces (**Figure 2.6**). After adding the PFPP lubricant on the anti-CD34 functionalized surfaces, endothelial cell attachment was investigated at two different time points (6 and 48 hours) following cell seeding. After each incubation time, the number of cells adhered to the surfaces were counted using fluorescence imaging and the average cell number per mm^2 was calculated. Surfaces blocked with BSA only were also investigated and the results were compared with 100% TPFS-PFPP surfaces.

As seen in **Figure 2.6a**, after 6 hours of cell seeding, in the CVD treated group, 100% APTES (0% TPFS) surfaces had significantly more cells adhered to their surface compared to other treatment groups (220 ± 23 cells/mm^2). Samples treated with 95% APTES (5% TPFS) and 75% APTES (25% TPFS) had 55 ± 12 and 67 ± 16 cells/mm^2 attached to their surfaces and no significant difference was seen between these two groups. Samples treated with 50% APTES (50% TPFS) and 100% TPFS had significantly lower amount of cells adhesion (less than 10 cells/mm^2) and these two surfaces prevented cell attachment and cell growth when compared to other samples. The low number of cells observed in the 50% APTES (50% TPFS) samples correlates with the low amount of anti-CD34 antibody immobilized on these surfaces. When comparing the surfaces

treated with the mixed ratios of APTES and TPFS with the BSA blocked surfaces, mixed silane surfaces had significantly lower cells compared to the BSA blocked surfaces. This indicates that in addition to having biofunctional properties, mixed silane treated surfaces exhibit better blocking properties compared to BSA treated samples.

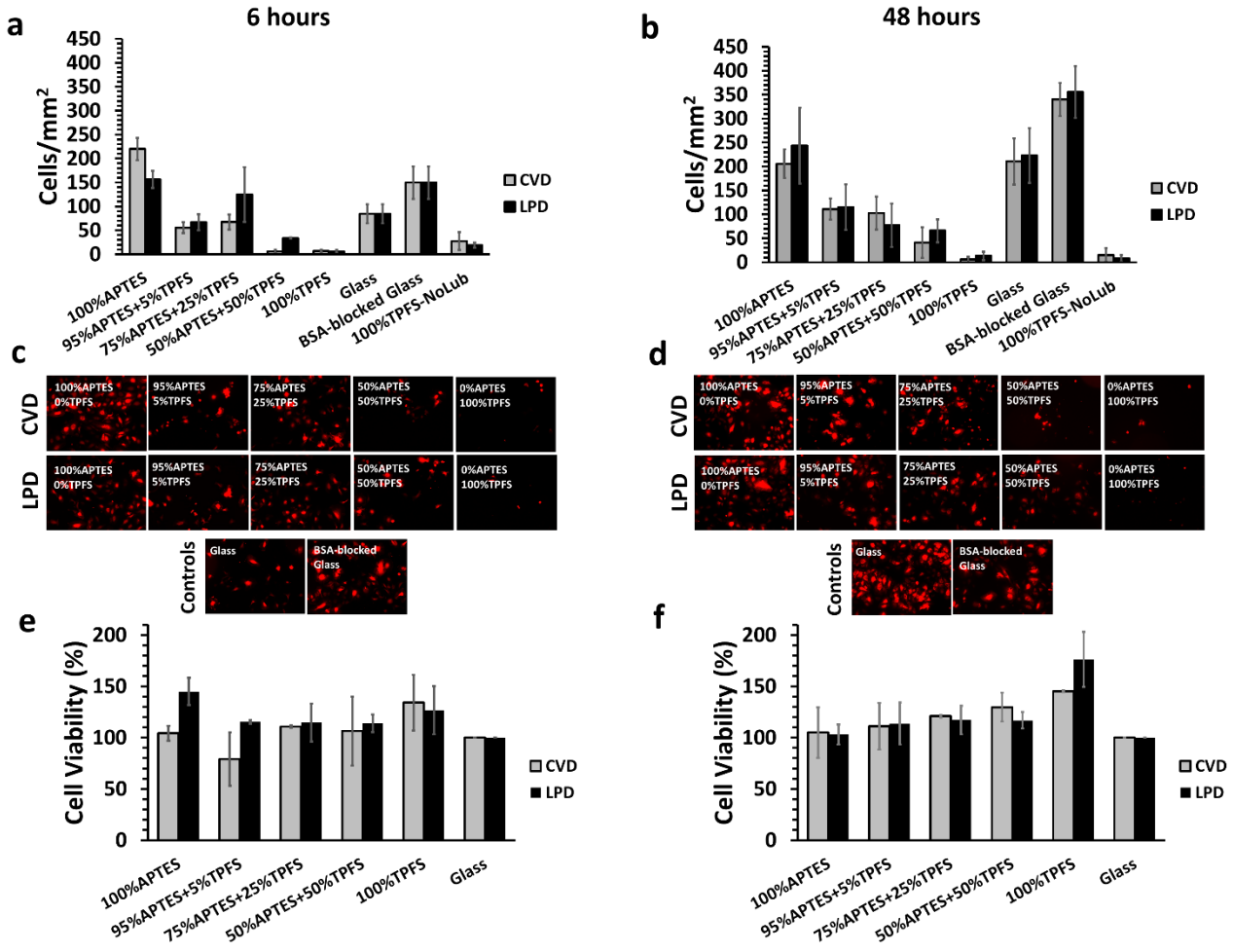

Figure 2.6. RFP-HUVEC attachment on CD34 treated and control samples and MTT assay. a) and **b)** In both CVD and LPD treated samples, cell count per mm^2 area was highest in 100% APTES samples which corresponds to the presence of a higher density of anti-CD34 antibody. 100% TPFS samples showed minimum amount of cell attachment, confirming the omniphobic slippery properties the lubricant infused surfaces and that these samples are protein and cell repellent and could be used as efficient blockers in biological environments. As the APTES to TPFS ratio decreases in the samples, the amount of cells attached to the surface decrease as well. This result is in line with the CD34 fluorescent intensity obtained from different samples. **c** and **d)** Representative fluorescent images with 10X magnification of RFP-HUVEC attachment to the surfaces are shown. **e** and **f)** The cell proliferation rates of RFP-HUVECs incubated for 6 or 48 hours with the treated and control surfaces were high and no significant decrease in cell viability was observed upon exposing RFP-HUVECs to the silanized and control samples.

After 48 hours of incubating CVD treated samples, the number of cells adhered to the glass substrates increased compared to the 6 hours incubated samples, but the same trend was seen when comparing the cell number of different silane ratios. Similar to the results obtained from 6 hours of cell seeding time, 100 % APTES (0% TPFS) treated surfaces had significantly more cells (206 ± 30 cells/mm^2) adhered to their surface compared to other treated groups. No significant difference was seen when comparing 95% APTES (5% TPFS) and 75% APTES (25% TPFS) samples (111 ± 22 and 103 ± 34 cells/mm^2 respectively). The 50% APTES (50% TPFS) retained their repellency properties after 48 hours by having a significantly lower amount of cells on their surfaces compared to other mixed silane ratios. Samples treated with 100% TPFS had the lowest amount of cells on their surfaces (6 ± 6 cells/mm^2) and showed excellent cell repellency even after 48 hours. Similar to previous studies, these results confirm that TPFS-PFPP surfaces can sufficiently prevent cell and protein adhesion and treated samples remained cell repellent even after 48 hours of incubation (Badv et al., 2017; Jiaxuan Chen et al., 2016; Leslie et al., 2014). In addition, surfaces that were treated with a ratio of mixed silanes, had significantly improved cell repellency properties compared to surfaces blocked with BSA. Similar to results obtained after 6 hours of incubation, surfaces treated with BSA did not show cell repellency properties.

In the LPD treated group, after 6 hours of incubation, similar to CVD treated samples, substrates treated with 100% APTES had the highest number of cells (156 ± 18 cells/mm^2) compared to other silane ratios. However, no significant difference was seen when comparing these results with the number of cells adhered to 95% APTES (5% TPFS) and 75% APTES (25% TPFS) treated samples. Samples treated with 75% APTES (25% TPFS) had a higher number of cells when compared with 95% APTES (5% TPFS) treated samples (125 ± 57, 67 ± 17, respectively), but the differences were not significant. 100% TPFS treated samples in the LPD group, also had high cell repellency

properties and acted better than the BSA blocked surfaces by having significantly lower number of cells adhered to their surface (6 ± 3 and 150 ± 34 cells/mm^2 respectively). Similar to the CVD treated group, samples treated with 50% APTES (50% TPFS) also showed cell repellency properties compared to other mixed silane ratios.

After 48 hours of cell incubation, similar to CVD treated samples, the number of cells had increased on all the LPD treated samples. The 100% TPFS lubricated surface showed excellent cell repellency even after 48 hours and all samples treated with different ratios of APTES to TPFS, except for 50% APTES (50% TPFS) samples, had significantly higher amount of cells compared to 100% TPFS samples. Samples treated with 100% APTES had a significantly higher amount of cells compared to other silane treated surfaces. Samples treated with 50% APTES (50% TPFS) remained cell repellent even after 48 hours and no significant difference was seen when comparing the results from this group with samples treated with 100% TPFS. The BSA blocked surfaces remained cell friendly after 48 hours and the number of cells in this group was significantly higher compared to 100% TPFS samples. Overall, there was no significant difference between the number of cells when comparing the LPD and CVD treated groups after 48 hours of cell seeding.

Samples blocked with BSA had significantly higher number of cells on their surface when compared to 100% TPFS-PFPP treated surfaces from both CVD and LPD treated groups. This shows that omniphobic lubricant infused surfaces produced by fluorinated TPFS molecules act as excellent blocking agents compared to the conventional BSA blocking system and adding the functional groups through aminosilanes provides control over the population of attached cells and does not compromise the repellency properties of these surfaces.

3.6. Cytotoxicity properties of treated glass substrates

The cytotoxicity of the treated surfaces was evaluated using the MTT assay at two different incubation times (6 and 48 hours). As seen in **Figure 2.6e** and **Figure 2.6f**, the cell proliferation rates of RFP-HUVECs incubated for 6 or 48 hours with the treated and control surfaces were high and no significant decrease in cell viability was observed upon exposing RFP-HUVECs to the silanized and control samples. This confirms that the produced biofunctional omniphobic coating is not toxic to cells and does not alter cell's viability.

4. Conclusion

In this work we have reported a method for successfully creating surfaces that are both biofunctional and capable of preventing non-specific adhesion of biomolecules and cells. Different ratios of TPFS and APTES were used in this study in order to obtain the optimized surface properties where modified substrates remained omniphobic and slippery while having biofunctional domains integrated onto their surfaces. Both methods of CVD and LPD treatment showed promising results, however the results obtained using the CVD method were more consistent and we were able to better control the physical and chemical properties of the modified surfaces obtained using this technique by tuning the ratios between APTES and TPFS molecules. Overall, the proposed technique is a straightforward and simple method that could be used to create biofunctional, lubricant infused surfaces for different applications such as medical implants and biosensors, where both biofunctionality and prevention of non-specific adhesion are key features that are required when utilizing these devices.

5. References

Acres, R. G., Ellis, A. V., Alvino, J., Lenahan, C. E., Khodakov, D. A., Metha, G. F., & Andersson, G. G. (2012). Molecular structure of 3-aminopropyltriethoxysilane layers formed on silanol-terminated silicon surfaces. *Journal of Physical Chemistry C*, *116*(10), 6289–6297. https://doi.org/10.1021/jp212056s

Anderson, A. S., Dattelbaum, A. M., Montano, G. A., Price, D. N., Schmidt, J. G., Martinez, J. S., … Swanson, B. I. (2008). Functional PEG-modified thin films for biological detection. *Langmuir*, *24*(5), 2240–2247. https://doi.org/10.1021/la7033438

Arima, Y., & Iwata, H. (2007). Effect of wettability and surface functional groups on protein adsorption and cell adhesion using well-defined mixed self-assembled monolayers. *Biomaterials*, *28*(20), 3074–3082. https://doi.org/10.1016/j.biomaterials.2007.03.013

Awsiuk, K., Bernasik, A., Kitsara, M., Budkowski, A., Petrou, P., Kakabakos, S., … Raptis, I. (2012). Spectroscopic and microscopic characterization of biosensor surfaces with protein/amino-organosilane/silicon structure. *Colloids and Surfaces B: Biointerfaces*, *90*(1), 159–168. https://doi.org/10.1016/j.colsurfb.2011.10.017

Awsiuk, K., Budkowski, A., Psarouli, A., Petrou, P., Bernasik, A., Kakabakos, S., … Raptis, I. (2013). Protein adsorption and covalent bonding to silicon nitride surfaces modified with organo-silanes: Comparison using AFM, angle-resolved XPS and multivariate ToF-SIMS analysis. *Colloids and Surfaces B: Biointerfaces*, *110*, 217–224. https://doi.org/10.1016/j.colsurfb.2013.04.030

Badv, M., Jaffer, I. H., Weitz, J. I., & Didar, T. F. (2017). An omniphobic lubricant-infused coating produced by chemical vapor deposition of hydrophobic organosilanes attenuates clotting on catheter surfaces. *Scientific Reports*, *7*(1), 11639. https://doi.org/10.1038/s41598-017-12149-1

Camci-Unal, G., Aubin, H., Ahari, A. F., Bae, H., Nichol, J. W., & Khademhosseini, A. (2010). Surface-modified hyaluronic acid hydrogels to capture endothelial progenitor cells. *Soft Matter*, *6*(20), 5120–5126. https://doi.org/10.1039/c0sm00508h

Castner, D. G., & Ratner, B. D. (2002). *Biomedical surface science: Foundations to frontiers*. *Surface Science* (Vol. 500). https://doi.org/10.1016/S0039-6028(01)01587-4

Chen, J., Cao, J., Wang, J., Maitz, M. F., Guo, L., Zhao, Y., … Huang, N. (2012). Biofunctionalization of titanium with PEG and anti-CD34 for hemocompatibility and stimulated endothelialization. *Journal of Colloid and Interface Science*, *368*(1), 636–647. https://doi.org/10.1016/j.jcis.2011.11.039

Chen, J., Howell, C., Haller, C. A., Patel, M. S., Ayala, P., Moravec, K. A., … Chaikof, E. L. (2016). An immobilized liquid interface prevents device associated bacterial infection in vivo. *Biomaterials*, *113*, 80–92. https://doi.org/10.1016/j.biomaterials.2016.09.028

Didar, T. F., Foudeh, A. M., & Tabrizian, M. (2012). Patterning multiplex protein microarrays in a single microfluidic channel. *Analytical Chemistry*, *84*(2), 1012–1018. https://doi.org/10.1021/ac2025877

Epstein, A. K., Wong, T.-S., Belisle, R. a, Boggs, E. M., & Aizenberg, J. (2012). Liquid-infused

structured surfaces with exceptional anti-biofouling performance. *Proceedings of the National Academy of Sciences of the United States of America*, *109*(33), 13182–13187. https://doi.org/10.1073/pnas.1201973109

Filippini, P., Rainaldi, G., Ferrante, A., Mecheri, B., Gabrielli, G., Bombace, M., … Santini, M. T. (2001). Modulation of osteosarcoma cell growth and differentiation by silane-modified surfaces. *Journal of Biomedical Materials Research*, *55*(3), 338–349. https://doi.org/10.1002/1097-4636(20010605)55:3<338::AID-JBM1022>3.0.CO;2-N

Gautrot, J. E., Huck, W. T. S., Welch, M., & Ramstedt, M. (2010). Protein-resistant NTA-functionalized polymer brushes for selective and stable immobilization of histidine-tagged proteins. *ACS Applied Materials and Interfaces*, *2*(1), 193–202. https://doi.org/10.1021/am9006484

Jang, L. S., & Liu, H. J. (2009). Fabrication of protein chips based on 3-aminopropyltriethoxysilane as a monolayer. *Biomedical Microdevices*, *11*(2), 331–338. https://doi.org/10.1007/s10544-008-9239-7

Jeyachandran, Y. L., Mielczarski, E., Rai, B., & Mielczarski, J. A. (2009). Quantitative and qualitative evaluation of adsorption/desorption of bovine serum albumin on hydrophilic and hydrophobic surfaces. *Langmuir*, *25*(19), 11614–11620. https://doi.org/10.1021/la901453a

Jönsson, U., Olofsson, G., Malmqvist, M., & Rönnberg, I. (1985). Chemical vapour deposition of silanes. *Thin Solid Films*, *124*(2), 117–123. https://doi.org/10.1016/0040-6090(85)90253-6

Kim, D. J., Lee, J. M., Park, J. G., & Chung, B. G. (2011). A self-assembled monolayer-based micropatterned array for controlling cell adhesion and protein adsorption. *Biotechnology and Bioengineering*, *108*(5), 1194–1202. https://doi.org/10.1002/bit.23029

Kim, J., Cho, J., Seidler, P. M., Kurland, N. E., & Yadavalli, V. K. (2010). Investigations of chemical modifications of amino-terminated organic films on silicon substrates and controlled protein immobilization. *Langmuir*, *26*(4), 2599–2608. https://doi.org/10.1021/la904027p

Kim, P., Wong, T. S., Alvarenga, J., Kreder, M. J., Adorno-Martinez, W. E., & Aizenberg, J. (2012). Liquid-infused nanostructured surfaces with extreme anti-ice and anti-frost performance. *ACS Nano*, *6*(8), 6569–6577. https://doi.org/10.1021/nn302310q

Leslie, D. C., Waterhouse, A., Berthet, J. B., Valentin, T. M., Watters, A. L., Jain, A., … Ingber, D. E. (2014). A bioinspired omniphobic surface coating on medical devices prevents thrombosis and biofouling. *Nature Biotechnology*, *32*(11), 1134–40. https://doi.org/10.1038/nbt.3020

Li, Q. L., Huang, N., Chen, C., Chen, J. L., Xiong, K. Q., Chen, J. Y., … Liang, X. (2010). Oriented immobilization of anti-CD34 antibody on titanium surface for self-endothelialization induction. *Journal of Biomedical Materials Research - Part A*, *94*(4), 1283–1293. https://doi.org/10.1002/jbm.a.32812

Liu, Y., & Yu, J. (2016). Oriented immobilization of proteins on solid supports for use in biosensors and biochips: a review. *Microchimica Acta*, *183*(1), 1–19.

https://doi.org/10.1007/s00604-015-1623-4

Liu, Z. Z., Wang, Q., Liu, X., & Bao, J. Q. (2008). Effects of amino-terminated self-assembled monolayers on nucleation and growth of chemical vapor-deposited copper films. *Thin Solid Films*, *517*(2), 635–640. https://doi.org/10.1016/j.tsf.2008.07.030

Lung, C. Y. K., & Matinlinna, J. P. (2012). Aspects of silane coupling agents and surface conditioning in dentistry: An overview. *Dental Materials*, *28*(5), 467–477. https://doi.org/10.1016/j.dental.2012.02.009

Qin, M., Hou, S., Wang, L., Feng, X., Wang, R., Yang, Y., … Qiao, M. (2007). Two methods for glass surface modification and their application in protein immobilization. *Colloids and Surfaces B: Biointerfaces*, *60*(2), 243–249. https://doi.org/10.1016/j.colsurfb.2007.06.018

Rusmini, F., Zhong, Z., & Feijen, J. (2007). Protein immobilization strategies for protein biochips. *Biomacromolecules*, *8*(6), 1775–1789. https://doi.org/10.1021/bm061197b

Spargo, B. J., Testoff, M. A., Nielsen, T. B., Stenger, D. A., Hickman, J. J., & Rudolph, A. S. (1994). Spatially controlled adhesion, spreading, and differentiation of endothelial cells on self-assembled molecular monolayers. *Proceedings of the National Academy of Sciences of the United States of America*, *91*(23), 11070–4. https://doi.org/10.1073/pnas.91.23.11070

Truskey, G. A., & Proulx, T. L. (1993). Relationship between 3T3 cell spreading and the strength of adhesion on glass and silane surfaces. *Biomaterials*, *14*(4), 243–254. https://doi.org/10.1016/0142-9612(93)90114-H

Tsai, W.-B., Chen, Y.-H., & Chien, H.-W. (2009). Collaborative Cell-Resistant Properties of Polyelectrolyte Multilayer Films and Surface PEGylation on Reducing Cell Adhesion to Cytophilic Surfaces. *Journal of Biomaterials Science-Polymer Edition*, *20*(11), 1611–1628. https://doi.org/10.1163/092050609x12464345178248

Wang, P., Zhang, D., Sun, S., Li, T., & Sun, Y. (2017). Fabrication of Slippery Lubricant-Infused Porous Surface with High Underwater Transparency for the Control of Marine Biofouling. *ACS Applied Materials & Interfaces*, *9*(1), 972–982. https://doi.org/10.1021/acsami.6b09117

Wang, W., & Vaughn, M. W. (2008). Morphology and amine accessibility of (3-aminopropyl) triethoxysilane films on glass surfaces. *Scanning*, *30*(2), 65–77. https://doi.org/10.1002/sca.20097

Wong, T.-S., Kang, S. H., Tang, S. K. Y., Smythe, E. J., Hatton, B. D., Grinthal, A., & Aizenberg, J. (2011). Bioinspired self-repairing slippery surfaces with pressure-stable omniphobicity. *Nature*, *477*(7365), 443–7. https://doi.org/10.1038/nature10447

Yin, M., Yuan, Y., Liu, C., & Wang, J. (2009). Combinatorial coating of adhesive polypeptide and anti-CD34 antibody for improved endothelial cell adhesion and proliferation. *Journal of Materials Science: Materials in Medicine*, *20*(7), 1513–1523. https://doi.org/10.1007/s10856-009-3715-3

Zhang, F., Sautter, K., Larsen, A. M., Findley, D. A., Davis, R. C., Samha, H., & Linford, M. R. (2010). Chemical vapor deposition of three aminosilanes on silicon dioxide: Surface characterization, stability, effects of silane concentration, and cyanine dye adsorption.

Langmuir, *26*(18), 14648–14654. https://doi.org/10.1021/la102447y

Chapter 3

Micropatterned Biofunctional Lubricant-Infused Surfaces Promote Selective Cell Adhesion and Patterning

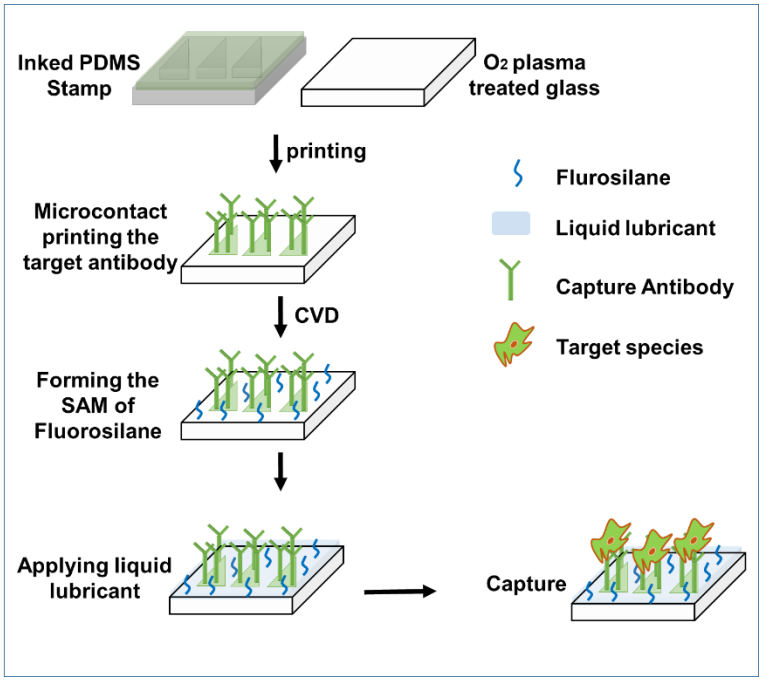

In chapter 3, all the experiments were conducted by myself and Maryam Badv who worked with me as a PhD student. Darren Yip and Claire Fine who were summer students of Didar Lab, helped with the Protein A section of this paper. My advisor, Prof. Didar gave me many helpful suggestions in both experiments and data analysis. I wrote the first draft of the paper together with Maryam Badv. Prof. Didar, helped me in revising the draft to the final version.

Micropatterned Biofunctional Lubricant-Infused Surfaces Promote Selective Cell Adhesion and Patterning

Sara M. Imani[1,Ψ], Maryam Badv[1,Ψ], Darren Yip[2], Claire Fine[3], Tohid F. Didar[1,4,5]

[1]School of Biomedical Engineering, McMaster University, Hamilton, Ontario, Canada.
[2]W Booth School of Engineering Practice and Technology, McMaster University, Hamilton, Ontario, Canada
[3]Department of Chemical Engineering, McMaster University, Hamilton, Ontario, Canada.
[4]Department of Mechanical Engineering, McMaster University, Hamilton, Ontario, Canada.
[5]Institute for Infectious Disease Research (IIDR), McMaster University, Hamilton, Ontario, Canada

[Ψ]***These authors contributed equally to this work.***

Correspondence author:

Tohid F. Didar, PhD

Department of Mechanical Engineering and School of Biomedical Engineering, McMaster University

1280 Main Street West, JHE-308A, Hamilton, Ontario, Canada, L8S 4L7

Ph: +1-905-5259140 Ex. 20413, fax: +1-905-572-7944

Email: didar@mcmaster.ca

Abstract

Micropatterned biofunctional surfaces have several applications in bioengineering. Among different methods of micropatterning biomolecules, microcontact printing proteins is a straightforward method for producing micropatterned biofunctional surfaces. A key characteristic which is sought for in these types of surfaces is prevention of non-specific adhesion for an enhanced biofunctionality. In this work, we developed a micropatterned omniphobic lubricant-infused surface by microcontact printing proteins on the surface and further producing self-assembled monolayers (SAMs) of fluorosilanes on the surface. First, micropatterns of FITC-

labeled protein A was created and blocked with our proposed method and then by incubating a rhodamine-labeled secondary antibody specific to protein A, biofunctionality of the samples as well as the specificity was evaluated. Furthermore, we created micropatterns of anti-CD34 antibody which is an endothelial cell specific ligand and then produced the SAMs of fluorosilanes to create a micropatterned biofunctional lubricant-infused surface. To evaluate the biofunctionality and the extent and specificity of the cells' adhesion, samples were incubated with red fluorescent protein expressing human umbilical vein endothelial cells (RFP-HUVEC). Furthermore, our proposed blocking method was compared to a conventional blocking method, Bovine Serum Albumin (BSA). The micropatterned omniphobic biofunctional surfaces demonstrated localised and specific adherence of the cells to the patterns, whereas, BSA-blocked surfaces showed randomly attached cells.

1. Introduction

Micropatterned biofunctional surfaces produced by patterning micro and nano size features of biomolecules (*e.g.* proteins) have several applications in biosensing, tissue engineering and Lab on Chip devices (Alom Ruiz & Chen, 2007; A Bernard, Renault, Michel, Bosshard, & Delamarche, 2000; Blawas & Reichert, 1998; Didar & Tabrizian, 2010; Kane, Takayama, Ostuni, Ingber, & Whitesides, 1999; W. Liu, Li, & Yang, 2013). The ability to pattern biomolecules leads to patterning cells which creates platforms for basic cell studies, single cell studies, tissue engineering, and also developing advanced implants (Blawas & Reichert, 1998; Falconnet, Csucs, Michelle Grandin, & Textor, 2006; Filipponi, Livingston, Kašpar, Tokárová, & Nicolau, 2016; Kasemo & Gold, 1999; Khademhosseini, Suh, & Zourob, 2011; Yokoyama, Matsui, & Deguchi, 2014).

There are several methods to pattern proteins on a desired substrate and photolithography is one of the most extensively used methods for this end (Blawas & Reichert, 1998; Truskett & Watts, 2006). Generally, in this technique, through an initial patterning with a photoresist and further functionalizing the patterned substrate with self-assembled monolayers (SAM) of molecules such as silanes, an anchorage pattern is created for proteins to bond (Blawas & Reichert, 1998; W.-D. Liu & Yang, 2017; Mrksich, Dike, Tien, Ingber, & Whitesides, 1997; Quist & Oscarsson, 2010). Generating samples with this method, requires clean room environments, using harsh solvents and also, costs highly, thus, making it inconvenient (Kane et al., 1999; Mrksich et al., 1997; Quist & Oscarsson, 2010). Microcontact printing (μCP), is another technique to pattern proteins and it was firstly introduced for formation of SAMs of alkanethiols (Kumar & Whitesides, 1993) and is based on an elastomeric stamp for pattern transfer and an ink which is the molecule printed on the surface. Later on, microcontact printing of proteins were introduced (James et al., 1998) which physically deposits the protein molecules on the surface and does not involve any harsh chemical in compare to conventional photolithographic methods and it is not expensive and relatively easy to perform (Kane et al., 1999).

One of the major issues with protein patterning is non-specific binding (A Bernard et al., 2000; Blawas & Reichert, 1998; Zhanga et al., 1999) which in case of protein microcontact printing, it is mainly tackled by further surface treatments with proteins such as bovine serum albumin (BSA) (A Bernard et al., 2000; Andre Bernard et al., 1998; Didar, Foudeh, & Tabrizian, 2012; Falconnet et al., 2006; MacBeath & Schreiber, 2000; Perl, Reinhoudt, & Huskens, 2009). However, BSA has been proven not to be stable on the surface, as it is physically immobilized (Falconnet et al., 2006; Rusmini, Zhong, & Feijen, 2007). Recently, omniphobic lubricant-infused surfaces have been introduced as an alternative for surface blocking. These surfaces have the capacity to repel various

liquids and are proven to be robust and durable coatings (Epstein, Wong, Belisle, Boggs, & Aizenberg, 2012; Kim et al., 2012; Leslie et al., 2014a; Wong et al., 2011). Lubricant-infused surfaces consist of self-assembled monolayers of a fluorinated silane (*e.g.* trichloro(1H,1H,2H,2H-perfluorooctyl)silane (TPFS)) which is infused by a perfluorocarbon lubricating liquid such as perfluoroperhydrophenanthrene (PFPP) (Badv, Jaffer, Weitz, & Didar, 2017; Leslie et al., 2014a). Furthermore, these surfaces have shown successful anti-biofouling performance (Epstein et al., 2012; Wang, Zhang, Sun, Li, & Sun, 2017) and anti-thrombogenic characteristics (Badv et al., 2017; Leslie et al., 2014a), therefore, they have made omniphobic lubricant-infused surfaces a promising coating to prevent non-specific binding of biomolecules.

In this study we set out to develop protein micropatterned lubricant-infused surfaces. First, we developed lubricant-infused glass surfaces with micropatterned FITC-labeled protein A and demonstrated that the developed surface maintained omniphobic properties. Moreover, biofunctionality of the surfaces were tested by incubating a rhodamine-labeled secondary antibody specific to protein A.

Furthermore, we developed micropatterned lubricant infused surfaces patterned with an endothelial cell specific ligand, anti-CD34, to investigate red fluorescent protein expressing human umbilical vein endothelial cells (RFP-HUVEC) adhesion. Here we demonstrate that the developed surfaces possess simultaneous repellency and biofunctionality and were able to create desired patterns of cells with localised cell adhesion with improved control over cell adhesion which results in an enhanced cell specific attachment.

2. Materials and methods

2.1. Materials

Trichloro (1H,1H,2H,2H-perfluorooctyl) silane (TPFS), (3-Aminopropyl)triethoxysilane (APTES), Phosphate Buffered Saline (PBS), Bovine Serum Albumin (BSA), perfluoroperhydrophenanthrene (PFPP) and protein A (FITC) were purchased from Sigma–Aldrich (Oakville, Canada). Red Fluorescent Protein Expressing Human Umbilical Vein Endothelial Cells (RFP-HUVEC) were generously provided by Dr. P. Ravi Selvaganapathy's lab at McMaster University. Cell media kit (EGM-2 BelletKit) and Trypsin neutralizing agent where purchased from Cedarlane (Burlington, Canada). Trypsin-EDTA (0.25%), phenol red was purchased from Thermo Fisher Scientific (Waltham, United States). Plain vista vision microscope slides were purchased from VWR (Radnor, United States). Anti-Protein A antibody (rhodamine) was purchased from Fitzgerald industries international (Acton, United states).

2.2. Oxygen plasma treatment of glass slides

Prior to microcontact printing of the proteins and silanizing them with TPFS, microscope glass slides were cut into small pieces using a handheld glass cutter and then, placed in an oxygen plasma cleaner (Harrick Plasma Cleaner, PDC-002, 230V). They were exposed to high-pressure oxygen plasma for 2 minutes to activate their surfaces with hydroxyl (OH) groups (**Figure 3.1**).

2.3. Microcontact printing of proteins

Polydimethylsiloxane (PDMS) stamps were fabricated using soft lithography and were used for microcontact printing. After rinsing the stamps with 70% (v/v) ethanol and drying them with air, 10 µL of 0.01 mM FITC-labeled protein A or anti-CD34 antibody solution was placed on the stamp and a pre plasma-treated cover slip was placed on top of the 10 µL droplet to evenly spread the protein on the PDMS stamp (**Figure 3.1**). Further, the coverslip was removed and the stamp

was washed with PBS and DI water, dried under nitrogen gas, and placed on top of a plasma-treated glass slide for 2 min in order to initiate the µCP of the protein (antibody) on the glass slide. All samples were visualized using a fluorescence microscope.

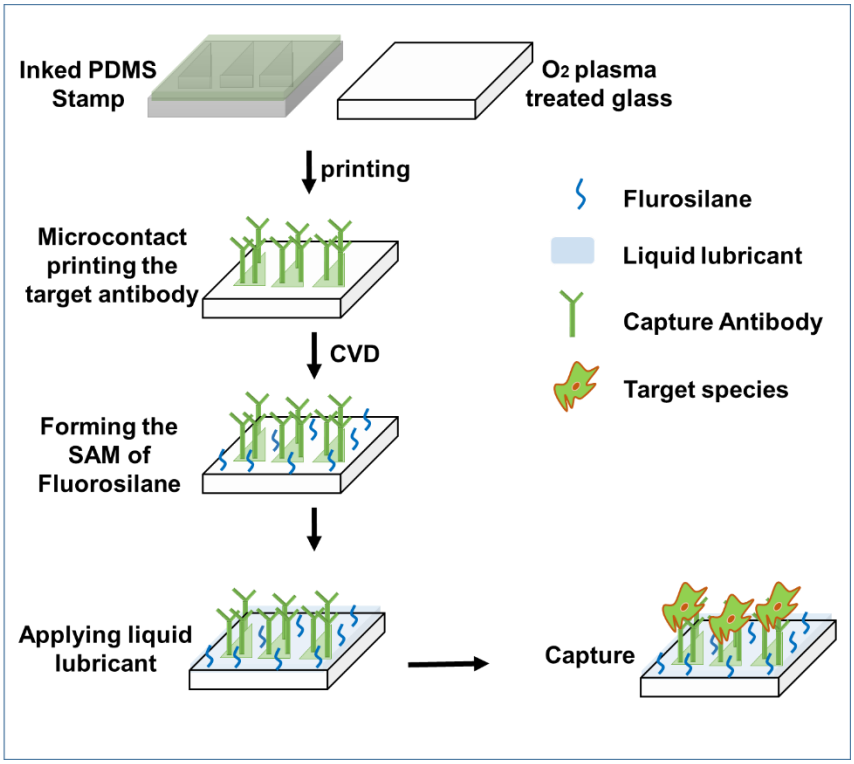

Figure 3.1. Schematic representation of creating a patterned biofunctional omniphobic lubricant infused surface using chemical vapor deposition (CVD) and microcontact printing (µCP). The oxygen plasma treated glass slides were first microcontact printed by a biomolecule, in this case fluorescently labelled anti-CD34 monoclonal antibody. Furthermore, treated with TPFS using the CVD method. After treating the samples, liquid lubricant was added to create the omniphobic lubricant-infused surfaces and further on, HUVECs where seeded on the samples.

2.4. Silanizing the µCP slides and producing TPFS layer using chemical vapor deposition (CVD)

To coat the patterned surface with TPFS using CVD, after removing the PDMS stamp from the glass slides, the printed surfaces were incubated in a desiccator with 200 µL of TPFS for 2 hours under vacuum. The CVD was initiated under vacuum with a pressure of – 0.08 MPA. Once the CVD treatment was completed, the glass samples were removed from the desiccator and placed in an oven at 37°C overnight.

2.5. Applying fluorinated lubricant on silanized samples

As a final step, before preforming different measurements on µCP-TPFS treated samples, glass slides were saturated with 100 µL of fluorinated lubricant in order to complete the surface modification process and to create microcontact printed omniphobic slippery surfaces. Perfluoroperhydrophenanthrene (PFPP) was the lubricant used in all experiments.

2.6. Characterization of the omniphobic properties – Contact and Sliding angle measurements

In order to investigate the omniphobic properties of the µCP-TPFS samples, their contact and sliding angles were measured using a 5µL droplet of deionized water. After µCP and silanizing the glass slide, water sessile drop contact angles were measured using Future Digital Scientific OCA20 goniometer (Garden City, NY). Prior to performing the measurements, the goniometer was calibrated. A digital angle level (ROK, Exeter, UK) was used in order to measure the sliding angles of the treated samples. µCP-TPFS samples saturated with PFPP were placed on the calibrated level and a 5µL droplet of deionized water was placed on their surfaces. Further, the surface which the glass slides were placed on was gently tilted and the sliding of the droplet was observed. Once the droplet would start moving on the glass surface, the angle was recorded as the minimum sliding angle. A sliding angle of 90 degrees was assigned to samples that the droplet would adhere to their surface and would not start to slide. All measurements were performed on three different surfaces and the means were calculated.

2.7. Evaluating the biofunctionality

The biofunctionality and ability of the µCP-TPFS-PFPP surfaces to prevent non-specific adhesion was investigated using two techniques. (i) Secondary protein adhesion on protein A printed samples (ii) RFP-HUVEC growth on anti-CD34 antibody printed samples.

2.7.1. Anti-protein A antibody adhesion

Samples printed using protein A and silanized with TPFS were lubricated with PFPP and incubated with 100 µL of 0.01 mM of anti-protein A antibody solution for 2 hours. Samples were then washed with PBS and DI water and were imaged using a fluorescence microscope in order to confirm the attachment of anti-protein A antibody to protein A patterns and to investigate the protein repellency of the non-patterned areas blocked with omniphobic lubricant infused monolayers.

2.7.2. Cell growth and cell adhesion

RFP-HUVEC's were seeded on samples that were microcontact printed using anti-CD34 antibody and cell attachment and growth was monitored after 6 and 24 hours. Briefly, anti-CD34 antibody printed glass samples were placed in wells of a 12 well plate and 1 mL of cell solution, with a concentration of 1.5 x 10^5 cells/mL was added to each well and cell containing plates were placed in a 5% CO_2 incubator at 37 °C. RFP-HUVECs of passage 4-6 were used for cell studies. Prior to adding the cells, PFPP was added to TPFS treated glass samples. After 6 and 24 hours incubation times, samples were imaged using fluorescence microscopy. Microcontact printed surfaces blocked using BSA and TPFS with no PFPP were investigated as controls as well as microcontact printed surfaces with no blocking. The results obtained from these surfaces were compared with surfaces blocked with TPFS-PFPP.

2.8. Statistical Analysis

All data are presented as means ± S.D. Each experiment condition was repeated at least three times. To access statistical significance between different groups, one-way analysis of variance (ANOVA) followed by post hoc analysis using Tukey's test was performed. P values less than 0.05 were considered statistically significant for all comparisons.

3. Results and Discussion

3.1. Producing protein A and anti-CD34 antibody patterned surfaces

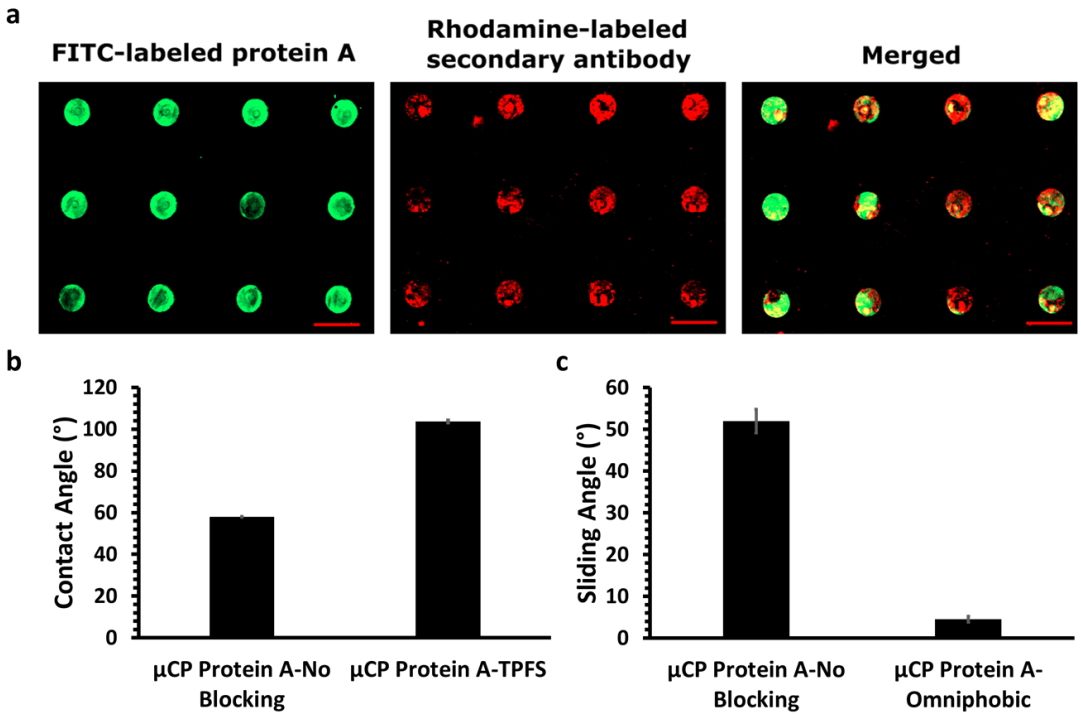

Figure 3.2. Verification of biofunctionality and omniphobicity of produced surfaces. a) Representative images of microcontact printed protein A on a glass substrate, immunoassay using a secondary antibody specific to protein A on the omniphobic surface, and superimposed image. Scale bar: 100 µm. **b and c)** Sliding angle and contact angle of biofunctional and biofunctional omniphobic glass slides.

Prior to blocking the surface with blocking agents, patterns of protein A or anti-CD34 antibody were microcontact printed on pre-oxygen plasma treated glass surfaces. **Figure 3.2a** and **Figure 3.3a** show the fluorescence patterns of protein A (circles) and anti-CD34 antibody (triangles) on a glass substrate respectively. As seen in the **Figures 3.2a** and **Figure 3.3a**, well-defined and clean patterns were generated using the printing technique and minimal amounts of protein A or antibody were deposited on non-patterned areas.

3.2. Contact and sliding angle measurements on printed and silanized surfaces

The omniphobic slippery properties of the patterned surfaces blocked using TPFS+PFPP were evaluated by performing contact and sliding angle measurements (**Figure 3.2b,c** and **Figure 3.3b,c**).

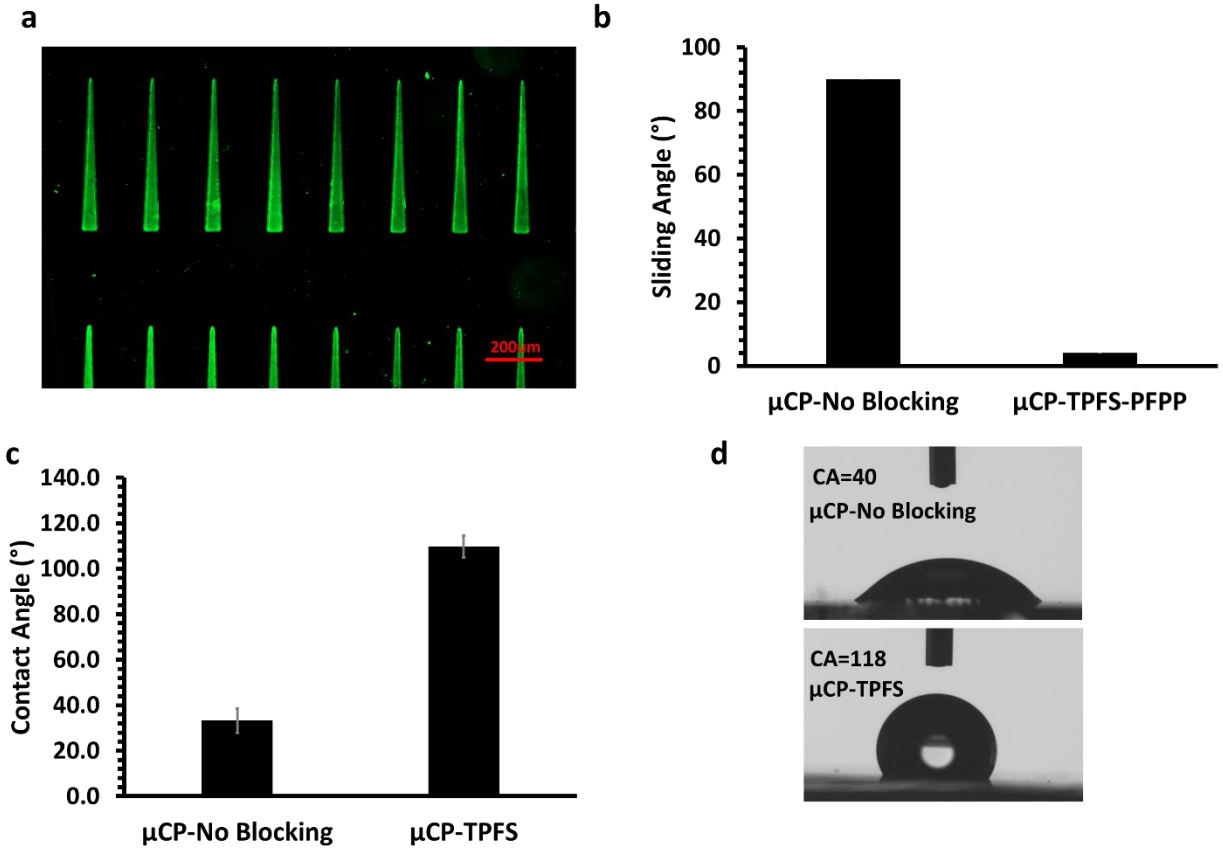

Figure 3.3. **Fluorescent image of a microcontact printed sample and verification of omniphobicity of the treated samples. a)** The oxygen plasma treated glass slides were microcontact printed by fluorescently labelled anti-CD34 monoclonal antibody. **b)** Fluorosilane treated and microcontact printed samples were lubricated and a 5 uL droplet was placed on the surface of the samples and the sliding angle was measured by lifting the surface and recording the angle which the droplet starts to move. **c)** Static Contact angle of the surfaces were measured prior to lubricating the surfaces (The results are presented as means ± SD). **d)** Representative images of the contact angle measurements.

Sliding angle measurements of the treated and control µCP samples are shown in **Figure 3.2** and **Figure 3.3**. Both protein A and anti-CD34 antibody µCP samples with no silanization, did not allow the water droplet to slide and the sliding angles were greater than 90 °. These surfaces did

not have omniphobic slippery properties. Whereas the microcontact printed, omniphobic lubricant-infused samples (μCP-TPFS-PFPP surface) showed an immediate sliding and movement of the water droplet (less than 5 °) and although these surfaces had hydrophilic protein features printed on them, they showed excellent water repellency properties. The results obtained from sliding angle measurements were comparable to previously reported lubricant infused surfaces (Badv et al., 2017; Leslie et al., 2014b).

The static contact angle measurements of the treated and control μCP samples are shown in **Figure 3.2d** and **Figure 3.3c**. Samples printed with anti-CD34 antibody or protein A were hydrophilic and exhibited low contact angles of 33.2±5.2 and 57.9 ± 0.2 respectively. Since the protein features on anti-CD34 antibody printed samples were bigger than the protein A printed samples, anti-CD34 printed samples had a lower contact angle and were more hydrophilic compared to protein A printed samples. After CVD treating the samples and adding the TPFS monolayer on the μCP surfaces, the contact angles elevated to 109.8±4.8 and 103.6 ± 0.7, and these surfaces showed the presences of the hydrophobic TPFS layer. There was no significant difference between the sliding angles of the protein A and anti-CD34 antibody printed surfaces.

3.3. Attachment of RFP-HUVECs on patterned surfaces and surface non-specific attachment properties

To demonstrate and compare the capability of the patterned surfaces to specifically capture cells, RFP-HUVECs were seeded on control, BSA, TPFS, and TPFS-PFPP CD34-printed samples and incubated for 6 and 24 hours in order for them to grow on the substrates. **Figure 3.4a** and **Figure 3.4b**, exhibit superimposed fluorescence microscope images of the cells and patterns, indicating how the cell have grown on the patterned substrates after 6 and 24 hours with different blocking agents.

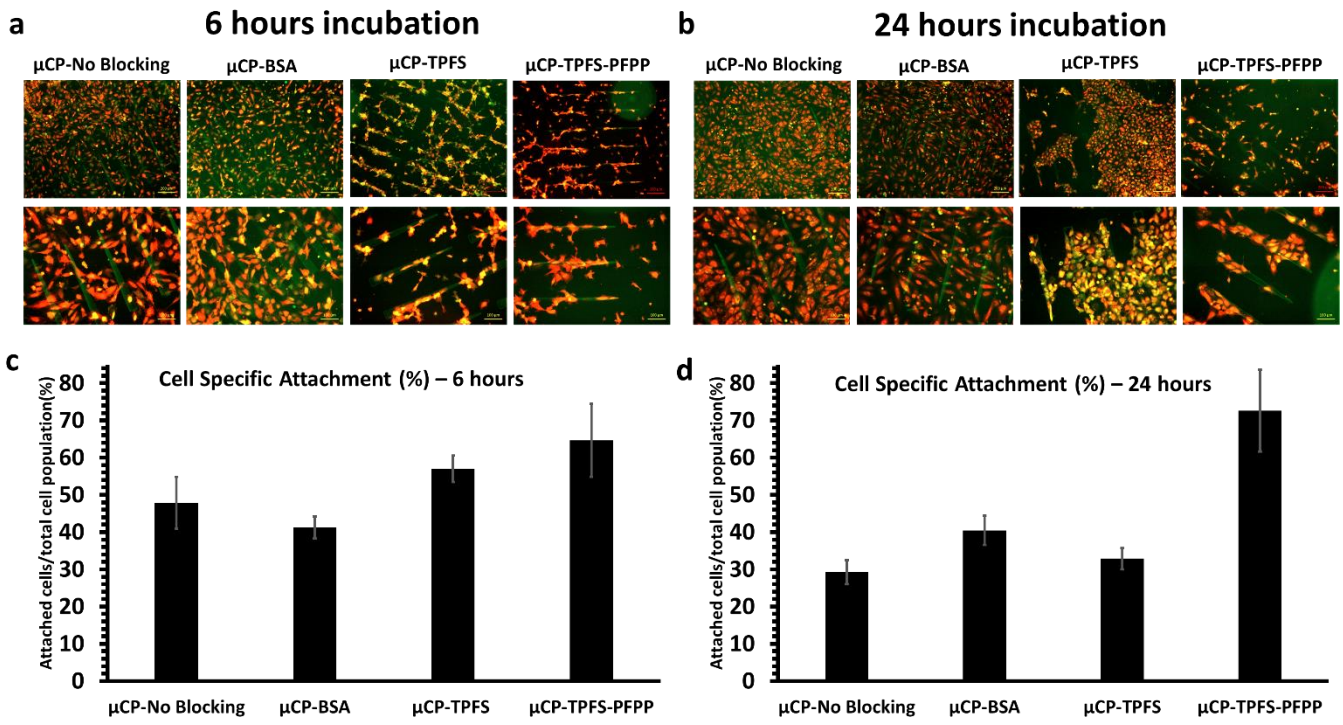

Figure 3.4. **RFP-HUVEC attachment on CD34 microcontact printed samples and quantifying the ratio of the HUVECs attached to CD34 microcontact printed features versus all the cells available in an identical area for each condition. a)** 6 hours of incubation. **b)** 24 hours of incubation. **c)** Cell Specific Attachment (%) after 6 hours. **d)** Cell Specific Attachment (%) after 24 hours.

Quantification of the ratio of the HUVECs attached to CD34 microcontact printed regions versus all the cells available in an identical area for each condition, are shown in **Figure 3.4c** and **Figure 3.4d**. HUVECs' attachment to µCP-TPFS-PFPP samples demonstrates a high specificity with 72.6% and 64.6% specific attachment of the cell population to the printed regions after 24 and 6 hours, respectively (**Figure 3.4c** and **Figure 3.4d**). Furthermore, in **Figure 3.4a** and **Figure 3.4b**, the µCP-TPFS-PFPP samples exhibit elongated cells in the direction of the pattern and also, within the area of the patterns.

µCP-BSA and µCP-TPFS surfaces which their blocking agents have previously been used in various studies (Camci-Unal et al., 2010; Lin et al., 2010; Spargo et al., 1994), show randomly attached cells to the surface due to the low attachment percentages of cells to the features after 24 hours of incubation (40.5% and 32.9%, respectively) which are comparable to our control µCP

samples with no blocking showing 29.3% cell specific attachment. In the same incubation time, μCP-TPFS-PFPP samples show a higher cell specific attachment of 72.6% in compare to those of μCP-BSA and μCP-TPFS surfaces.

μCP-TPFS surfaces show a superior blocking performance in 6 hours (57%) compared to 24 hours incubation (32.9%), which can indicate short term blocking capabilities of this blocking agent. BSA, however, does not act well as a blocking agent after 6 hours of incubation, since the cell specific attachment percentage is 41.25% which is in the range of control μCP samples with no blocking (47.8%). In the same incubation time, μCP-TPFS-PFPP samples, demonstrate 64.6% cell specific attachment percentage which indicates an improved performance than the other control samples.

4. Conclusion

In summary, omniphobic lubricant infused surfaces were successfully applied to biofunctional microcontact printed surfaces and they showed excellent water and cell repellency properties. Surfaces coated with TPFS and PFPP outperformed conventional blocking systems such as BSA and remained repellent even after being incubated with cells for 24 h. Cells were mainly aligned along the anti-CD34 antibody patterns on surfaces blocked using TPFS and PFPP while surfaces blocked with BSA or surfaces with no blocking had random cell attachment and cell orientation. In conclusion, in this work we showed omniphobic lubricant infused coatings could successfully be integrated with microcontact printing techniques in order to act as blocking agents and to prevent non-specific adhesion of cells and biomolecules.

5. References

Alom Ruiz, S., & Chen, C. S. (2007). Microcontact printing: A tool to pattern. *Soft Matter*, *3*(2), 168–177. https://doi.org/10.1039/B613349E

Badv, M., Jaffer, I. H., Weitz, J. I., & Didar, T. F. (2017). An omniphobic lubricant-infused coating produced by chemical vapor deposition of hydrophobic organosilanes attenuates clotting on catheter surfaces. *Scientific Reports*, *7*(1), 11639. https://doi.org/10.1038/s41598-017-12149-1

Bernard, A., Delamarche, E., Schmid, H., Michel, B., Bosshard, H. R., & Biebuyck, H. (1998). Printing patterns of proteins. *Langmuir*, *14*(9), 2225–2229. https://doi.org/10.1021/la980037l

Bernard, A., Renault, J. P., Michel, B., Bosshard, H. R., & Delamarche, E. (2000). Microcontact printing of proteins. *Advanced Materials*, *12*(14), 1067–1070. https://doi.org/Doi 10.1002/1521-4095(200007)12:14<1067::Aid-Adma1067>3.0.Co;2-M

Blawas, A. S., & Reichert, W. M. (1998). Protein patterning. *Biomaterials*, *19*(7–9), 595–609. https://doi.org/10.1016/S0142-9612(97)00218-4

Camci-Unal, G., Aubin, H., Ahari, A. F., Bae, H., Nichol, J. W., & Khademhosseini, A. (2010). Surface-modified hyaluronic acid hydrogels to capture endothelial progenitor cells. *Soft Matter*, *6*(20), 5120–5126. https://doi.org/10.1039/c0sm00508h

Didar, T. F., Foudeh, A. M., & Tabrizian, M. (2012). Patterning multiplex protein microarrays in a single microfluidic channel. *Analytical Chemistry*, *84*(2), 1012–1018. https://doi.org/10.1021/ac2025877

Didar, T. F., & Tabrizian, M. (2010). Adhesion based detection, sorting and enrichment of cells in microfluidic Lab-on-Chip devices. *Lab on a Chip*, *10*(22), 3043. https://doi.org/10.1039/c0lc00130a

Epstein, A. K., Wong, T.-S., Belisle, R. a, Boggs, E. M., & Aizenberg, J. (2012). Liquid-infused structured surfaces with exceptional anti-biofouling performance. *Proceedings of the National Academy of Sciences of the United States of America*, *109*(33), 13182–13187. https://doi.org/10.1073/pnas.1201973109

Falconnet, D., Csucs, G., Michelle Grandin, H., & Textor, M. (2006). Surface engineering approaches to micropattern surfaces for cell-based assays. *Biomaterials*, *27*(16), 3044–3063. https://doi.org/10.1016/j.biomaterials.2005.12.024

Filipponi, L., Livingston, P., Kašpar, O., Tokárová, V., & Nicolau, D. V. (2016). Protein patterning by microcontact printing using pyramidal PDMS stamps. *Biomedical Microdevices*, *18*(1), 1–7. https://doi.org/10.1007/s10544-016-0036-4

James, C. D., Davis, R. C., Kam, L., Craighead, H. G., Isaacson, M., Turner, J. N., & Shain, W. (1998). Patterned Protein Layers on Solid Substrates by Thin Stamp Microcontact Printing. *Langmuir*, *14*(4), 741–744. https://doi.org/10.1021/la9710482

Kane, R. S., Takayama, S., Ostuni, E., Ingber, D. E., & Whitesides, G. M. (1999). Patterning proteins and cells using soft lithography. *Biomaterials*, *20*(23–24), 2363–2376.

https://doi.org/10.1016/S0142-9612(99)00165-9

Kasemo, B., & Gold, J. (1999). Implant surfaces and interface processes. *Advances in Dental Research*, *13*(v), 8–20. https://doi.org/10.1177/08959374990130011901

Khademhosseini, A., Suh, K.-Y., & Zourob, M. (2011). Biological Microarrays. *Methods in Molecular Biology (Clifton, N.J.)*, *671*(3), 336. https://doi.org/10.1007/978-1-59745-551-0

Kim, P., Wong, T. S., Alvarenga, J., Kreder, M. J., Adorno-Martinez, W. E., & Aizenberg, J. (2012). Liquid-infused nanostructured surfaces with extreme anti-ice and anti-frost performance. *ACS Nano*, *6*(8), 6569–6577. https://doi.org/10.1021/nn302310q

Kumar, A., & Whitesides, G. M. (1993). Features of gold having micrometer to centimeter dimensions can be formed through a combination of stamping with an elastomeric stamp and an alkanethiol "ink" followed by chemical etching. *Applied Physics Letters*, *63*(14), 2002–2004. https://doi.org/10.1063/1.110628

Leslie, D. C., Waterhouse, A., Berthet, J. B., Valentin, T. M., Watters, A. L., Jain, A., … Ingber, D. E. (2014a). A bioinspired omniphobic surface coating on medical devices prevents thrombosis and biofouling. *Nature Biotechnology*, *32*(11), 1134–40. https://doi.org/10.1038/nbt.3020

Leslie, D. C., Waterhouse, A., Berthet, J. B., Valentin, T. M., Watters, A. L., Jain, A., … Ingber, D. E. (2014b). A bioinspired omniphobic surface coating on medical devices prevents thrombosis and biofouling. *Nature Biotechnology*, *32*(11), 1134–40. https://doi.org/10.1038/nbt.3020

Lin, Q., Ding, X., Qiu, F., Song, X., Fu, G., & Ji, J. (2010). In situ endothelialization of intravascular stents coated with an anti-CD34 antibody functionalized heparin-collagen multilayer. *Biomaterials*, *31*(14), 4017–4025. https://doi.org/10.1016/j.biomaterials.2010.01.092

Liu, W.-D., & Yang, B. (2017). Patterned surfaces for biological applications: A new platform using two dimensional structures as biomaterials. *Chinese Chemical Letters*, *28*(4), 675–690. https://doi.org/10.1016/j.cclet.2016.09.004

Liu, W., Li, Y., & Yang, B. (2013). Fabrication and applications of the protein patterns. *Science China Chemistry*, *56*(8), 1087–1100. https://doi.org/10.1007/s11426-013-4909-6

MacBeath, G., & Schreiber, S. L. (2000). Printing proteins as microarrays for high-throughput function determination. *Science*, *289*(September), 1760–1763. https://doi.org/10.1126/science.289.5485.1760

Mrksich, M., Dike, L. E., Tien, J., Ingber, D. E., & Whitesides, G. M. (1997). Using microcontact printing to pattern the attachment of mammalian cells to self-assembled monolayers of alkanethiolates on transparent films of gold and silver. *Experimental Cell Research*, *235*(2), 305–313. https://doi.org/10.1006/excr.1997.3668

Perl, A., Reinhoudt, D. N., & Huskens, J. (2009). Microcontact printing: Limitations and achievements. *Advanced Materials*, *21*(22), 2257–2268. https://doi.org/10.1002/adma.200801864

Quist, A. P., & Oscarsson, S. (2010). Micropatterned surfaces: techniques and applications in cell biology. *Expert Opinion on Drug Discovery*, *5*(September), 569–581. https://doi.org/10.1517/17460441.2010.489606

Rusmini, F., Zhong, Z., & Feijen, J. (2007). Protein immobilization strategies for protein biochips. *Biomacromolecules*, *8*(6), 1775–1789. https://doi.org/10.1021/bm061197b

Spargo, B. J., Testoff, M. A., Nielsen, T. B., Stenger, D. A., Hickman, J. J., & Rudolph, A. S. (1994). Spatially controlled adhesion, spreading, and differentiation of endothelial cells on self-assembled molecular monolayers. *Proceedings of the National Academy of Sciences of the United States of America*, *91*(23), 11070–4. https://doi.org/10.1073/pnas.91.23.11070

Truskett, V. N., & Watts, M. P. C. (2006). Trends in imprint lithography for biological applications. *Trends in Biotechnology*, *24*(7), 312–317. https://doi.org/10.1016/j.tibtech.2006.05.005

Wang, P., Zhang, D., Sun, S., Li, T., & Sun, Y. (2017). Fabrication of Slippery Lubricant-Infused Porous Surface with High Underwater Transparency for the Control of Marine Biofouling. *ACS Applied Materials & Interfaces*, *9*(1), 972–982. https://doi.org/10.1021/acsami.6b09117

Wong, T.-S., Kang, S. H., Tang, S. K. Y., Smythe, E. J., Hatton, B. D., Grinthal, A., & Aizenberg, J. (2011). Bioinspired self-repairing slippery surfaces with pressure-stable omniphobicity. *Nature*, *477*(7365), 443–7. https://doi.org/10.1038/nature10447

Yokoyama, S., Matsui, T. S., & Deguchi, S. (2014). Microcontact peeling as a new method for cell micropatterning. *PLoS ONE*, *9*(7). https://doi.org/10.1371/journal.pone.0102735

Zhanga, S., Lin, Y., Altman, M., Lässle, M., Nugent, H., Frankel, F., … Rich, A. (1999). Biological surface engineering: A simple system for cell pattern formation. *Biomaterials*, *20*(13), 1213–1220. https://doi.org/10.1016/S0142-9612(99)00014-9

Chapter 4 – Conclusion and future works

In this work, we were able to successfully develop and design biofunctional omniphobic lubricant-infused interfaces by different means. In detail, conclusions and contribution of this work is as follows:

- Chapter 2:
    - Coating a surface with mixed SAMs of organosilanes and proving their presence and functionality by both CVD and LPD methods
    - Successful implementation of aminosilanes as an anchorage site for biomolecule immobilization and controlling the extent of it by prevention of non-specific binding at the same time
    - Controlling the degree of cell adhesion to the surface by changing the ratio of the mixed SAMs of organosilanes
- Chapter 3:
    - Production of a protein micropatterned surface by microcontact printing
    - Integrating omniphobic characteristics by producing SAMs of fluorosilanes on the surface
    - Successful localized and controlled cell attachment to the micropatterned features

Results of this work, can open up a platform for investigating new coatings for different bio-interfaces which require control over the degree of biological elements' attachment to the surface. For instance, there can be studies about transferring mixed SAMs of organosilanes to medical implants in order to enhance their anti-thrombogenic characteristics and at the same time, improve generation of cellular layer and their integration to human body. Our proposed micropatterned

omniphobic surfaces can be used in in different biological assays and cell capture studies. Following are suggested ideas and experiments for future works:

- Investigating blood coagulation and thrombosis on the developed surfaces using bioassays
- Investigating detection and capturing of target species (*e.g.* cells or pathogens) from complex fluids such as blood using the developed surfaces
- Transferring the developed coatings from the used substrates (glass) onto medical implants or biosensors for developing interfaces with higher specificity and sensitivity.